

Galerkin method for nanofluid flow over a stretching sheet



By

Izza Qamar

Supervised By

Dr. Muhammad Asif Farooq

A thesis

submitted in partial fulfillment of the
requirements for the degree of

Master of Science

in

Mathematics

Department of Mathematics

School of Natural Sciences,


National University of Sciences and Technology,

H-12, Islamabad, Pakistan

2022

National University of Sciences & Technology**MS THESIS WORK**

We hereby recommend that the dissertation prepared under our supervision by: IZZA QAMAR, Regn No. 00000331149 Titled: "Galerkin method for nanofluid flow over a stretching sheet" accepted in partial fulfillment of the requirements for the award of **MS** degree.

Examination Committee Members1. Name: DR. MERAJ MUSTAFA HASHMISignature: 2. Name: DR. MUJEEB UR REHMANSignature: Supervisor's Name: DR. MUHAMMAD ASIF FAROOQSignature: 
Head of Department30/08/2022
Date**COUNTERSIGNED**Date: 31.8.2022
Dean/Principal

My humble effort I dedicate to my

Parents

and

Brother

Acknowledgement

Foremost, I thank Allah Almighty for paving the way for me to achieve the milestone of completion of research work. It is His blessings that humbles and gratifies a person in the process of any accomplishment.

As daunting as the research thesis task sounds it is relatively made easier with the right guidance of the supervisor. As a novice learner in this field, I overcame the hindrances following the recommendations offered by my supervisor. Personally, I am obliged for the efforts made by my supervisor Dr. Muhammad Asif Farooq in order to construct a clear understanding of the concepts. I would like to extend my sincere thanks to him for his assistance at every stage of the research phase.

The timely completion of this work is attributed to my kind friends who have unhesitatingly supported me throughout to work with a clear and peaceful mind.

Lastly, but most importantly my parents who have supported me and have been a pillar of strength throughout my entire life. I am forever indebted to them for their selfless gestures.

Abstract

The thesis mainly discusses the influence of Arrhenius activation energy and variable thermal conductivity on EMHD flow of bionanofluid over a nonlinearly radiating stretching sheet in a porous medium. Considered partial differential equations (PDEs) for the described model is written into a system of nonlinear ordinary differential equations (ODEs) by using similarity transformations. The transformed ODEs are solved numerically by utilizing `bvp4c`, shooting method and Galerkin method that are implemented in MATLAB. We see an excellent agreement of FEM results with other numerical methods like shooting method and `bvp4c`. Graphical illustrations are provided to see the varying effects of relevant parameters.

Contents

1	Introduction	8
1.1	Literature review	8
1.2	Fluid	9
1.2.1	Fluid as a continuum	10
1.2.2	Newtonian fluid	10
1.2.3	Non-Newtonian fluid	10
1.2.4	Compressible flow	10
1.2.5	Incompressible flow	10
1.2.6	Steady and unsteady flow	11
1.2.7	Magnetohydrodynamics flow	11
1.3	Boundary layer	11
1.3.1	Momentum boundary layer	12
1.3.2	Thermal boundary layer	12
1.3.3	Concentration boundary layer	13
1.4	Conservation laws	13
1.4.1	Mass conservation law	13
1.4.2	Momentum conservation law	14
1.4.3	Energy conservation law	14
1.5	Dimensionless parameters	14
1.5.1	Magnetic parameter (M)	14
1.5.2	Porosity parameter (K_p)	14
1.5.3	Prandtl number (Pr)	15
1.5.4	Eckert number (Ec)	15
1.5.5	Brownian motion parameter (Nb)	15
1.5.6	Thermophoresis parameter (Nt)	15
1.5.7	Schmidt number (Sc)	16
1.5.8	Peclet number (Pe)	16

1.5.9	Biot number (Bi)	16
1.5.10	Reynolds number (Re)	16
1.5.11	Lewis number (Le)	16
1.6	Numerical methods	17
1.6.1	bvp4c	17
1.6.2	Shooting method	17
1.6.3	Finite element method (FEM)	19
2	Second grade convective nanofluid flow with buoyancy effect	21
2.1	Intoduction	21
2.2	Mathematical formulation	21
2.2.1	Skin friction coefficient	24
2.2.2	Local Nusselt number	24
2.2.3	Local Sherwood number	24
2.3	Numerical methodology	25
2.4	Discussion	26
3	Impact of Arrhenius activation energy on bionanofluid MHD flow with variable thermal conductivity over nonlinearly stretching sheet	35
3.1	Introduction	35
3.2	Mathematical formulation	35
3.2.1	Skin friction coefficient	39
3.2.2	Local Nusselt number	39
3.2.3	Local Sherwood number	40
3.2.4	Local density of motile microorganisms	40
3.3	Numerical Process	40
3.3.1	Linearization	40
3.3.2	Finite element method	42
3.3.3	Shooting method	44
3.3.4	bvp4c	45
3.4	Discussion	46
4	Conclusion	61

List of Tables

2.1	Influence of parameters on skin friction coefficient	27
2.2	Influence of parameters on local Nusselt number	28
2.3	Influence of parameters on local Sherwood number	28
3.1	Comparison of $-\theta'(0)$ for various values of Pr_0	46
3.2	Effect of different parameters on skin friction coefficient	47
3.3	Effect of different parameters on local Nusselt number	48
3.4	Effect of different parameters on local Sherwood number	50
3.5	Effect of different parameters on density for motile microorganisms	51

List of Figures

2.1	Computation of profile for velocity with respect to varied α_1 .	29
2.2	Computation of profile for velocity with respect to varied λ .	29
2.3	Computation of profile for velocity with respect to varied Nr .	30
2.4	Computation of profile for temperature with respect to varied Nb .	30
2.5	Computation of profile for temperature with respect to varied Nt .	31
2.6	Computation of profile for temperature with respect to varied Le .	31
2.7	Computation of profile for temperature with respect to varied Nr .	32
2.8	Computation of profile for concentration with respect to varied Nb .	32
2.9	Computation of profile for concentration with respect to varied Nt .	33
2.10	Computation of profile for concentration with respect to varied Le .	33
2.11	Computation of profile for concentration with respect to varied Nr .	34
3.1	Computation of profile for velocity with respect to varied M .	53
3.2	Computation of profile for velocity with respect to varied Kp .	53
3.3	Computation of profile for temperature with respect to varied Pr .	54
3.4	Computation of profile for temperature with respect to varied Rd .	54
3.5	Computation of profile for temperature with respect to varied Ec .	55
3.6	Computation of profile for temperature with respect to varied ϵ .	55
3.7	Computation of profile for temperature with respect to varied s .	56
3.8	Computation of profile for temperature with respect to varied β_1 .	56
3.9	Computation of profile for concentration with respect to varied δ .	57
3.10	Computation of profile for concentration with respect to varied E .	57
3.11	Computation of profile for concentration with respect to varied n .	58
3.12	Computation of profile for concentration with respect to varied Sc .	58
3.13	Computation of profile for concentration with respect to varied σ_1 .	59
3.14	Computation of profile for concentration with respect to varied β_2 .	59
3.15	Analysis of microorganisms profile $\chi(\eta)$ for varied Pe .	60
3.16	Analysis of microorganisms profile $\chi(\eta)$ for varied Sb .	60

Chapter 1

Introduction

1.1 Literature review

The study of fluid flow over a stretching sheet has wide range of applications. A sheet is moved with velocity in order to make the fluid flow. Nonlinearly stretching is described as when the sheet is stretched with non linear velocity.

Fluids are mostly used as cooling agents in most of cooling system. The base fluid with low thermal conductivity was a serious limitation to the heat transfer. With the immense technological advances made over the past few decades in different areas there was an increased need to address the thermal management issues. Therefore, the nanofluids were introduced. The term Nanofluid was first coined by Sir Stephen Choi in the 1995. Choi and Eastman showed that the thermal conductivity significantly increased when magnetic nanoparticles were suspended within the base fluid [1]. The nanoparticles ranging from size (1-100 *nm*) when dispersed uniformly within the basefluids produce nanofluids. Nanofluids are known for their enhanced thermophysical properties such as thermal conductivity and convective heat transfer than their base fluids [2]. Numerous applications of heat transfer includes vehicle cooling, electronic devices, paper production, atomic reactor and many more.

Due to the engineering and industrial applications, the analysis of flow and heat transfer past a stretching sheet has gained immense interest among researchers. Gupta et al. [3] inquired the heat and mass transfer with constant temperature of surface in a stretching problem. The evolution of the boundary layer flow induced merely due to the stretching sheet was first studied by Crane [4]. Heat transfer also occurs through thermal radiation. Variable fluid properties under the influence of thermal radiation are discussed in [5]. It has multiple applications in turbine, furnace design and solar collectors. On the other hand, the way buoyancy force influence the development of velocity and thermal boundary layer flow over a stretching sheet have been studied by Chen [6].

Various number of areas crucially base their work on the magnetic field such as magnetic resonance imaging (MRI), geothermal energy extractions and chemical engineering. Combine effect of both electric and magnetic flows for non-Newtonian nanofluids over a thin needle were discussed by Maqbool et al. [7].

Over time nanofluid appeared with difficulties. The instability of nanoparticles is often an issue adding to that mishandling, clogging, insufficient mixing of the sample resulting in reduction of heat and mass transfer rate [8]. In view of this, fluid having both nanoparticles and living microorganisms have been introduced. The living organisms in bionanfluid accounts for bioconvection. This phenomenon stabilizes the nanoparticles and enhances the thermal and mass transport susceptibility of the fluid [9]. Uddin et al. [10] explored the concept of bioconvection nanofluid over a curved surface pertaining to nano-biofuel cells. Aziz et al. [11] explored the nanofluids free convection flow with microorganisms. Bioconvection along with the suspension of nanoparticles is key in biotech, environmental systems and biomedical engineering.

Activation energy is the minimum energy required to reactants to undergo chemical transformation or physical transport. Arrhenius energy with mass transport phenomenon and chemical reaction has been widely analysed owing to its numerous advantages in compounds invention and geothermal artificial lake. To provide the activation energy through Arrhenius equation can be difficult at time as the temperature highly fluctuates with the rate constant. It is crucial to be effective with the reaction and energy discarded as the conversions can have diverse effect from reactants. Mustafa et al. [12] discussed the properties of magneto-nanofluid with Activation energy and buoyancy influence. In recent times, many efforts have been made in this regard as this emerging phenomenon has wide applications discussed in [13], [14] and [15].

1.2 Fluid

Solid, liquid and gas are three fundamental states in which a substance can exist. Anything in liquid or gas state is fluid. The distinction between the fluid and solid lies in the reaction to applied shear stress. A solid can resist the applied shear stress by static deformation whereas the fluid will result in motion regardless of how small the shear stress is. Fluid flow problems comes in a wide and different range. To make it easier fluid flow problems are categorized based on common characteristics.

1.2.1 Fluid as a continuum

When a material system comprises of continuous material and each particle is a continuum of matter, the system is said to be a continuum. The continuum hypothesis states that as the matter is made up of molecules, a large number of molecules are present in a small volume. Rather than to study the properties of individual particles in the continuum specifically fluid, we consider the average of the properties for a large number of molecules in vicinity of respective point(molecule). The averaging of properties for large molecules leads to the postulate for continuity, that is, the matter is continuously distributed in the whole imagined region, even in the smallest volumes, with a large number of molecules [16].

1.2.2 Newtonian fluid

The fluids that exhibit constant viscosity under different shear rates given that the temperature remains constant are known as Newtonian fluids. In other words, a fluid in which viscous stresses are linearly correlated with the local strain rate. The linear fluids which follows the following equation

$$\tau = \mu \frac{du}{dy}, \quad (1.1)$$

are called Newtonian fluids.

1.2.3 Non-Newtonian fluid

The fluids that violates the Newton's law for viscosity.

1.2.4 Compressible flow

The compressible flow of fluids occurs when the density of fluids change under pressure. Gases like air, oxygen, and nitrogen are commonly thought of as compressible fluids [17].

1.2.5 Incompressible flow

A fluid flow with almost constant density is known as incompressible flow. A flow in which every small volume of fluid that moves within it remains constant in density.

1.2.6 Steady and unsteady flow

The term steady reflects that there is no change in variable over time.

$$\frac{\partial \zeta}{\partial t} = 0. \quad (1.2)$$

The term unsteady means otherwise that there is change in given variable over time [18].

$$\frac{\partial \zeta}{\partial t} \neq 0. \quad (1.3)$$

1.2.7 Magnetohydrodynamics flow

The study of dynamics of electrically conductive fluids under the magnetic field is called Magnetohydrodynamics(MHD). When the conductive fluid is moving in the presence of magnetic field, then a current is induced by the magnetic field. The flow is modified considerably due to the affect of magnetic field on the current. Conversely, current modifies the magnetic field. Therefore, it is a complex interaction between fluid dynamic and magnetic phenomenon. It is dealt by considering equations of Navier-Stokes for fluid dynamics and Maxwell's equation of electromagnetism [19]. Anwar et al. [20] investigated the porous channel with generalized conditions having MHD flow. The Navier-Stokes equation for an MHD flow is as follows

$$\rho \frac{D\vec{V}}{Dt} = (\vec{J} \times \vec{B}) + \vec{\nabla} \cdot \tau, \quad (1.4)$$

where \vec{V} is the velocity vector, magnetic field is expressed as \vec{B} and \vec{J} denotes current density.

$$\vec{J} = \sigma(\vec{E} + \vec{V} \times \vec{B}),$$

where \vec{E} is the electric field and σ is the electrical conductivity. Lorentz force is given by

$$\vec{V} \times \vec{B} = B_0 u \hat{k}, \quad (1.5)$$

$$\vec{J} \times \vec{B} = -\sigma B_0^2 u \hat{i}. \quad (1.6)$$

1.3 Boundary layer

In 1904, Prandtl showed that it is possible to study viscous flows by dividing them into two regions: a region that has a thin layer of flow nearby a solid wall, which is called a boundary

layer that does not neglect viscous forces and an outer region that can ignore friction [21]. There are few assumptions considered for boundary layer. They are explained for continuity equation and momentum equation for two dimensional steady and incompressible flow. The velocity vector is defined as

$$\vec{v} = u(x, y)\hat{i} + v(x, y)\hat{j} \quad (1.7)$$

The continuity and momentum equation are

$$\begin{aligned} & u_x + v_y = 0, \\ x\text{-direction} \quad & \rho(uu_x + vu_y) = -P_x + \mu(u_{xx} + u_{yy}), \\ y\text{-direction} \quad & \rho(uv_x + vv_y) = -P_y + \mu(v_{xx} + v_{yy}), \end{aligned} \quad (1.8)$$

The assumptions are

$$u \gg v, \quad \frac{\partial}{\partial y} \gg \frac{\partial}{\partial x}, \quad (1.9)$$

The resulting equations are

$$\begin{aligned} \rho(uu_x + vu_y) &= -P_x + \mu u_{yy}, \\ P_y &= 0. \end{aligned} \quad (1.10)$$

1.3.1 Momentum boundary layer

To comply with the no slip condition, the fluid particles at the solid surface exhibit the zero velocity. Subsequently, they effect the velocity of fluid particles of adjacent layer and as result they further effect the velocity of adjacent fluid particles and so on. This process of slowing of velocity takes place at a certain distance from a flat surface. Fluid velocity in the boundary layer varies from 0 to $0.99U_\infty$, where free stream velocity is exhibited by U_∞ .

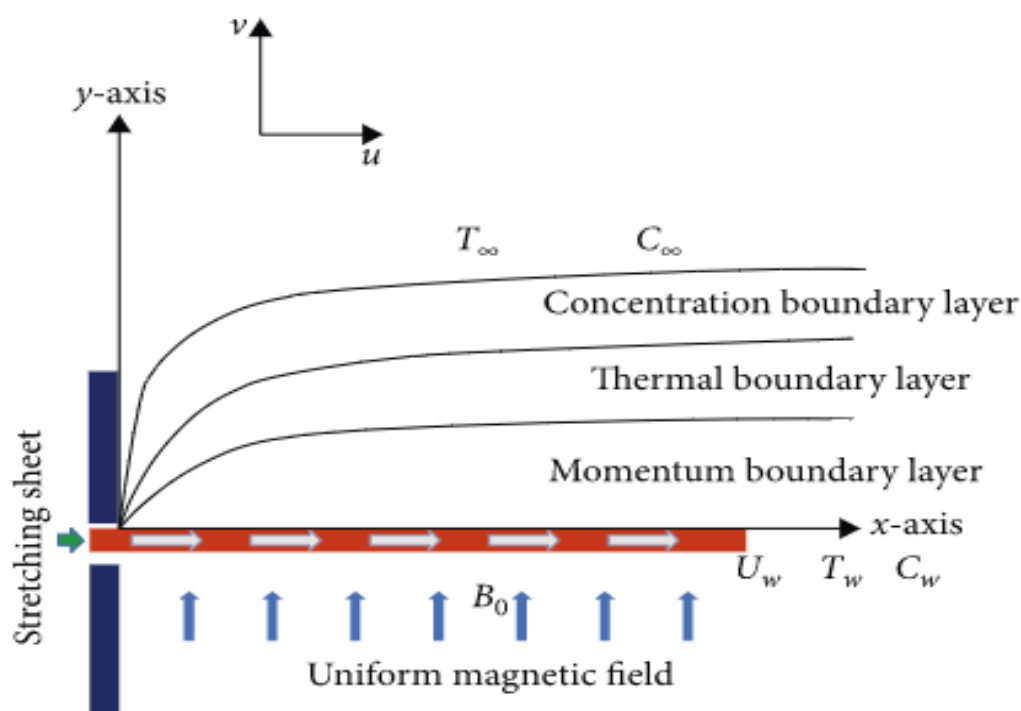
1.3.2 Thermal boundary layer

Consider the fluid flow over a heated surface that has higher temperature than the fluid. Consequently, the region of the fluid being heated by the surface is restricted to a thin layer near the surface and this region where the temperature field exists is called thermal boundary layer. Subsequently, when we move away from the heated surface, the temperature of the fluid drops until it becomes equal to that of free stream.

1.3.3 Concentration boundary layer

The boundary area when the concentration of nanofluid becomes closer to 99% of concentration of free stream.

The pictorial representation is given below and it is sourced from internet.



1.4 Conservation laws

1.4.1 Mass conservation law

The law states that mass can neither be created nor destroyed. The differential form for mass conservation is given by

$$\frac{\partial \rho}{\partial t} + \vec{\nabla} \cdot (\rho \vec{V}) = 0, \quad (1.11)$$

known as Continuity equation. The equation of continuity is reduced to following equation if flow is incompressible [22].

$$\nabla \cdot \vec{V} = 0. \quad (1.12)$$

1.4.2 Momentum conservation law

Newton's second law $\sum F = ma$, is the basis upon which the law of conservation of momentum is based upon. The rate of change in momentum of a body is equal to the force applied to it, according to the rule, and it happens in the same direction as the force. The conservation states that the momentum of system remains constant if no external force is applied.

$$\rho \frac{d\vec{V}}{dt} = \vec{\nabla} \cdot \tau + \rho \vec{g}, \quad (1.13)$$

where τ denotes the stress tensor and $\frac{d}{dt}$ represents the material time derivative.

1.4.3 Energy conservation law

Energy of the system remains constant although the form of the energy within a system is changed as it cannot be created or destroyed.

$$\rho C_p \frac{dT}{dt} = \vec{\nabla} \cdot (k \vec{\nabla} T) + \phi, \quad (1.14)$$

where k is the thermal conductivity, T is temperature, ϕ is the viscous dissipation function.

1.5 Dimensionless parameters

1.5.1 Magnetic parameter (M)

The ratio of Lorentz force to inertial force is the magnetic interaction parameter,

$$M = \frac{\sigma B_o^2}{\rho a}, \quad (1.15)$$

where B_o is the magnetic field strength, σ is the electrical conductivity, ρ is the density and a is the positive constant.

1.5.2 Porosity parameter (K_p)

Porosity parameter is the depiction of microstructures of the material. It is the percentage of the void spaces or pores to the total volume.

1.5.3 Prandtl number (Pr)

Prandtl number is expressed as the ratio between momentum diffusivity to thermal diffusivity.

$$Pr = \frac{\nu}{\alpha} = \frac{c_p \mu}{k}, \quad (1.16)$$

where k and c_p are the thermal conductivity and the specific heat respectively.

1.5.4 Eckert number (Ec)

The Eckert number expresses the link between flows kinetic energy and the boundary layer enthalpy difference to characterise heat transfer dissipation.

$$Ec = \frac{\text{Advective Transport}}{\text{Heat Dissipation}} = \frac{u^2}{c_p \Delta T}, \quad (1.17)$$

where u and c_p represent flow velocity and specific heat capacity respectively. The temperature difference is given by ΔT .

1.5.5 Brownian motion parameter (Nb)

The parameter that accounts for the random, haphazard motion of particles suspended in the fluid.

$$Nb = \frac{\tau D_B (C_w - C_\infty)}{\nu}, \quad (1.18)$$

where $\tau = \frac{(\rho c)_p}{(\rho c)_f}$ and D_B represents Brownian diffusion.

1.5.6 Thermophoresis parameter (Nt)

The parameter that accounts for the transport of particles due to the temperature gradient created because of fluid in contact with wall with difference in temperature is known as thermophoresis parameter.

$$Nt = \frac{\tau D_T (T_w - T_\infty)}{\nu T_\infty}, \quad (1.19)$$

where D_T represents thermophoretic diffusion.

1.5.7 Schmidt number (Sc)

Schmidt number is defined as the ratio between momentum diffusivity and mass diffusivity, which characterizes the fluid flows.

$$Sc = \frac{\text{Viscous Diffusion}}{\text{Mass Diffusion}} = \frac{\mu}{\rho D}, \quad (1.20)$$

where μ is the fluid dynamic viscosity, D is mass diffusivity and ρ is fluid density.

1.5.8 Peclet number (Pe)

The Peclet number represents the ratio between rate of convection to the diffusion rate in the convection and diffusion transport system.

$$Pe = \frac{\text{Convective transport rate}}{\text{Diffusive transport rate}}. \quad (1.21)$$

1.5.9 Biot number (Bi)

It represents the ratio between the resistance offered to heat transfer by the inside of the body to the external resistance.

$$Bi = \frac{\text{Internal conductive resistance}}{\text{External convective resistance}}. \quad (1.22)$$

1.5.10 Reynolds number (Re)

The Reynolds number refer to the ratio between inertial and viscous forces.

$$Re = \frac{\rho u L}{\mu}, \quad (1.23)$$

where u and L represents the flow velocity and characteristic length respectively.

1.5.11 Lewis number (Le)

The ratio between the thermal diffusion to the mass diffusion is represented by the Lewis number. It characterizes the fluid flows where the simultaneous occurrence of heat and mass transfer happens. Thus, it explains the relative thickness of thermal and concentration boundary layers.

$$Le = \frac{\text{Thermal diffusivity}}{\text{Mass diffusivity}} = \frac{\alpha}{D}, \quad (1.24)$$

where α is given thermal diffusivity and D is mass diffusivity.

1.6 Numerical methods

1.6.1 `bvp4c`

The `bvp4c` solver in MATLAB is an effective tool to solve fairly complex problems. For solving nonlinear systems of equations, the algorithm uses an iteration structure. It is based on collocation method. The residual of the continuous solution is used for mesh selection and error control. As `bvp4c` is an iterative method, the algorithm's effectiveness will ultimately be determined by the ability to make an initial guess for the solution. The MATLAB commands used are

$$soll = \text{bvp4c}(\text{odefun}, \text{bcfun}, \text{solinit}), \quad (1.25)$$

where `odefun` is the function of system of first order differential equations, `bcfun` indicates the boundary conditions under consideration and `solinit` forms the initial guess for the boundary value problem.

1.6.2 Shooting method

In numerical analysis, a boundary value problem is reduced to an initial value problem through a method called Shooting method. The name 'shoot' comes from the fact that in order to determine the needed initial condition, one shoot trajectories in different direction from one boundary until it hits the other boundary condition. Once the initial guess is chosen, the root-finding method is applied. Further procedure in practise is to convert the problem to the system of first order differential equations and solve numerically. A simple example of second order differential equation along with boundary conditions is solved below.

Consider a differential equation along with subjected boundary conditions. Use Euler's method with step size $h=3$

$$\begin{aligned} \frac{d^2y}{dx^2} - 2y &= 8x(9 - x), \\ y(0) &= 0, \quad y(9) = 0. \end{aligned} \quad (1.26)$$

The solution is mainly divided in four steps. Firstly, we solve the given differential equation with initial condition method which requires two initial conditions. To find the needed initial conditions we shoot our assumptions in different trajectories until it coincides with the relevant

boundary condition.

Let us consider an initial guess as λ_1 thus $y'(0) = \lambda_1$. Let $\lambda_1 = 4$, therefore problem now becomes

$$\begin{aligned}\frac{d^2y}{dx^2} &= 2y + 8x(9 - x), \\ y(0) &= 0, \quad y'(0) = 4.\end{aligned}$$

In the next step, we convert the second differential equation into the system of first order differential equations along with the initial condition.

$$\begin{aligned}\frac{dy}{dx} &= z = f_1(x, y, z), \\ \frac{dz}{dx} &= 2y + 8x(9 - x) = f_2(x, y, z).\end{aligned}\tag{1.27}$$

subjected to the initial conditions

$$y(0) = 0, \quad \frac{dy}{dx}(0) = 4.$$

In the next step, Euler's method is applied respectively to corresponding Eq. (1.27) as

$$\begin{aligned}Y_{i+1} &= f_1(X_i, Y_i, Z_i)h + Y_i, \\ Z_{i+1} &= f_2(X_i, Y_i, Z_i)h + Z_i.\end{aligned}\tag{1.28}$$

Following the calculations, we get

$$Y_3 = Y(9) = 1548 \neq y(9) = 0.$$

As the obtained solution is not the required root, we take another guess $y'(0) = \lambda_2$ and for this problem we take $\lambda_2 = 24$ and repeat the above procedure. The acquired solution using Euler's method is

$$Y_3 = Y(9) = -216 \neq y(9) = 0,$$

To better approximate the root we use Secant method. Substituting the values in

$Y'(0)$	$Y(3) \approx y(9)$
4	1548
-24	-216
p	q

$$p = p_0 + \frac{p_1 - p_0}{q_1 - q_0}(q - q_0).$$

We obtain the root as $p = y'(0) = 20.5$. Furthermore, we apply the Euler's method and solution is

i	X	Y
0	0	0
1	3	-61.71
2	6	-123.42
3	9	0.03

1.6.3 Finite element method (FEM)

It is a mathematical technique that is used to find the approximate solution of differential equations that occur in different fields such as engineering and applied sciences. Over time its use was expanded to the field of continuum mechanics which includes heat transfer and fluid flow.

To approximate the solution we here use weighted residual approach for FEM. We directly work on the governing equation. This method can be applied to linear and nonlinear problems. The method has two basic steps. Firstly, according to the general behaviour of the dependent variable, we suppose a trial function that should also satisfy the boundary conditions. Then, we substitute this assumed trial function into the governing differential equation. As this assumed solution is only an approximation of the exact solution, therefore, it will not satisfy the differential equation instead it will result into an error term generally called as residual. Now we need to vanish the residual over the whole domain. By doing this process, we will get a system of algebraic equations. Further step of this technique involves to get the solution of this system depending on the boundary conditions to get an estimated solution for the problem under consideration.

Different methods are based on this approach and one of them is Galerkin method. General steps for solving the differential equation with Galerkin method are explained below.

Let us consider a general second order differential equation along with subjected initial conditions where $x \in (x_0, x_n)$.

$$\frac{d^2u}{dx^2} + g_1 \frac{du}{dx} + g_2u = 0, \quad (1.29)$$

along with initial condition

$$u(0) = 0, \quad \left. \frac{du}{dx} \right|_{x=x_n} = u'.$$

In the initial step we assume an approximate solution of u denoted by \hat{u} . In the next step, we write the residual equation as we approximate the solution.

$$R = \frac{d^2\hat{u}}{dx^2} + g_1 \frac{d\hat{u}}{dx} + g_2\hat{u}. \quad (1.30)$$

For the Galerkin method, the basis function or interpolation is represented as the weight function $w_i(x)$.

By the method of weighted residual, we have

$$\int_{x_0}^{x_n} R(x)w_i(x) = 0, \quad (1.31)$$

Substiting Eq. (1.30) in the above Eq. (1.31) we obtain,

$$\int_{x_0}^{x_n} \left(\frac{d^2\hat{u}}{dx^2} + g_1 \frac{d\hat{u}}{dx} + g_2\hat{u} \right) w_i(x) = 0, \quad (1.32)$$

Using integration by parts on the first term of above Eq. (1.32), we obtain weak form

$$- \int_{x_0}^{x_n} \frac{d\hat{u}}{dx} \frac{dw_i}{dx} dx + \left[\frac{d\hat{u}}{dx} w_i \right]_{x_0}^{x_n} + \int_{x_0}^{x_n} \frac{d\hat{u}}{dx} g_1 w_i dx + \int_{x_0}^{x_n} \hat{u} g_2 w_i dx = 0,$$

Furthermore, we substitute the shape function. Shape functions have two important characteristics:

- The shape function corresponds to 1 at node i and 0 otherwise.

$$H_1(x_i) = 1, H_1(x_{i+1}) = 0, H_2(x_i) = 0, H_2(x_{i+1}) = 1.$$

- All shape functions add up to give unity.

$$\sum_{i=1}^2 H_i(x) = 1.$$

Subsequently we evaluate the integrals for each element. Then we substitute the values of evaluated integrals in the global matrix. Last step is to substitute the initial conditions and solve the obtained algebraic system of equations and hence the solution is obtained.

Chapter 2

Second grade convective nanofluid flow with buoyancy effect

2.1 Introduction

In this chapter, we explore the review problem which can be further seen in [23]. We discuss the influence on heat flux, mass transfer and solute distributions of buoyancy force in convective second grade nanofluid. We also consider the presence of Brownian diffusion, thermal diffusion and Newtonian heating. Subsequently, the similarity variable are used to transform partial differential equations to the ordinary differential equations. Moreover using the method of *bvp4c* on MATLAB the system of ordinary differential equations is solved. Furthermore, the effect of different parameters on skin friction coefficient, local Nusselt number and local Sherwood number is numerically examined and displayed in form of tables. The impact on profiles for velocity, temperature and concentration by variation of parameters are investigated and displayed through graphs.

2.2 Mathematical formulation

Second grade fluid flow is modelled considering the two dimensional laminar, steady and incompressible assumptions.

The fluid motion is caused by a stretching sheet with the velocity having components $w_x(x, t)$ and $w_y(x, t)$ in direction of x -axis and y -axis respectively.

Under the above assumptions and along with the boundary layer assumptions the system of

equations is given by Waqas et al. [24]:

$$\frac{\partial w_x}{\partial x} + \frac{\partial w_y}{\partial y} = 0, \quad (2.1)$$

$$w_x \frac{\partial w_x}{\partial x} + w_y \frac{\partial w_x}{\partial y} = \nu \frac{\partial^2 w_x}{\partial y^2} + \frac{\alpha_1^*}{\rho_f} \left(\frac{\partial w_x}{\partial x} \frac{\partial^2 w_x}{\partial y^2} + w_x \frac{\partial^3 w_x}{\partial y^2 \partial x} + \frac{\partial w_y}{\partial y} \frac{\partial^2 w_y}{\partial y^2} + w_y \frac{\partial^3 w_x}{\partial y^3} \right) + \frac{1}{\rho_f} [(1 - C_\infty) \rho_f g (T - T_\infty) \beta_T - g (C - C_\infty) (\rho_p - \rho_f)], \quad (2.2)$$

$$w_x \frac{\partial T}{\partial x} + w_y \frac{\partial T}{\partial y} = \alpha \frac{\partial^2 T}{\partial y^2} + \tau \left[D_B \frac{\partial T}{\partial y} \frac{\partial C}{\partial y} + \frac{D_T}{T_\infty} \left(\frac{\partial T}{\partial y} \right)^2 \right], \quad (2.3)$$

$$w_x \frac{\partial C}{\partial x} + \frac{\partial C}{\partial y} w_y = \frac{\partial^2 C}{\partial y^2} D_B + \frac{D_T}{T_\infty} \frac{\partial^2 T}{\partial y^2} - K_R (C - C_\infty). \quad (2.4)$$

Here, w_x represents the fluid velocity component parallel to x -axis and w_y represents fluid velocity component parallel to y -axis, τ represents specific heat capacity, ν exhibits kinematic viscosity, α gives the thermal diffusivity, α_1^* gives second grade parameter, β_T represents volume expansion fluid coefficient, c_p is the specific heat, D_T is the thermal diffusion coefficient, D_B represents the Brownian diffusion, temperature is represented by T , C expresses concentration distribution, T_W gives the wall temperature, C_W exhibits concentration at wall, K_R is used for chemical reaction.

The boundary conditions are:

$$w_x = U_w = ax, \quad w_y = V_w, \quad \frac{\partial T}{\partial y} = -h_s (T_w - T), \quad \frac{\partial C}{\partial y} = -h_c (C_w - C), \quad \text{at } y = 0, \quad (2.5)$$

$$w_x \rightarrow 0, \quad w_y \rightarrow 0, \quad T \rightarrow T_\infty, \quad C \rightarrow C_\infty, \quad \text{as } y \rightarrow y_\infty.$$

Here, U_w is fixed for velocity, V_w also represents velocity, h_s represents the heat transport coefficient, mass transport coefficient is represented by h_c , T_∞ gives the ambient temperature, C_∞ gives the ambient concentration.

The velocity components are defined as

$$w_x = U_w f'(\eta), \quad w_y = -\sqrt{a\nu} f(\eta). \quad (2.6)$$

The similarity variables are

$$\eta = \sqrt{\frac{a}{\nu}}y,$$

$$\theta = \frac{T - T_\infty}{T_w - T_\infty}, \quad (2.7)$$

$$\phi = \frac{C - C_\infty}{C_w - C_\infty}.$$

After applying the similarity transformation and using Eq. (2.6) - Eq. (2.7) the incompressibility condition Eq. (2.1) is trivially satisfied while Eq. (2.2) - Eq. (2.4) are reduced to

$$f''' + ff'' + \alpha_1(2f'f''' - (f'')^2 - ff^{(4)}) - (f')^2 + \lambda(\theta - Nr\phi) = 0, \quad (2.8)$$

$$\theta'' + NbPr\theta'\phi' + PrNt(\theta')^2 + Prf\theta' = 0, \quad (2.9)$$

$$\phi'' + Le f\phi' + \frac{Nt}{Nb}\theta'' - K_1\phi = 0. \quad (2.10)$$

Transformed boundary conditions are

$$f(0) = A, \quad f'(0) = 1, \quad \theta'(0) = -\gamma_1(1 - \theta(0)), \quad \phi'(0) = -\gamma_2(1 - \phi(0)), \quad (2.11)$$

$$f'(\infty) \rightarrow 0, \quad f''(\infty) \rightarrow 0, \quad \theta(\infty) \rightarrow 0, \quad \phi(\infty) \rightarrow 0.$$

The resulting parameters are

$$\alpha_1 = \frac{\alpha_1^* a}{\rho\nu}, \quad \lambda = \frac{(1 - C_\infty)\beta_T g(T_w - T_\infty)}{a^2 x}, \quad Nr = \frac{(C_w - C_\infty)(\rho_p - \rho_f)}{\rho_f(1 - C_\infty)\beta_T(T_w - T_\infty)},$$

$$\alpha = \frac{\nu}{Pr}, \quad Nt = \frac{\tau D_T(T_w - T_\infty)}{\nu T_\infty}, \quad Nb = \frac{\tau D_B(C_w - C_\infty)}{\nu},$$

$$Le = \frac{\nu}{D_B}, \quad A = \frac{-V_w}{\sqrt{a\nu}}, \quad \gamma_1 = h_s \sqrt{\frac{\nu}{a}}, \quad \gamma_2 = h_c \sqrt{\frac{\nu}{a}}.$$

Here, α_1 indicates the parameter for second grade fluid, Nr the buoyancy influence parameter, λ the mixed convection parameter, Nt the thermophoresis diffusion parameter, Nb represents the Brownian motion, Le is Lewis number, Pr is the Prandtl number, A is a suction/injection parameter, γ_1 and γ_2 are thermal and concentration Biot numbers respectively.

2.2.1 Skin friction coefficient

It is a dimensionless parameter and a function of Reynolds number Re . Defined as

$$Cf_x = \frac{(\tau_{xy})|_{y=0}}{\rho U_w^2}, \quad (2.12)$$

where,

$$\tau_{xy} = \mu \frac{\partial w_x}{\partial y} + \alpha_1^* (w_x \frac{\partial^2 w_x}{\partial y \partial x} + 2 \frac{\partial w_x}{\partial x} \frac{\partial w_x}{\partial y} + w_y \frac{\partial^2 w_x}{\partial y^2}), \quad (2.13)$$

Using Eq. (2.6) and Eq. (2.13) in Eq. (2.12) we get,

$$Cf(Re_x)^{\frac{1}{2}} = \alpha_1 (3f''(0) - Af'''(0)) + f''(0). \quad (2.14)$$

2.2.2 Local Nusselt number

The ratio of the heat transfer by convection and conductive heat transfer. It is a dimensionless parameter. Defining it as,

$$Nu_x = \frac{q_w x}{k_0 (T_w - T_\infty)}, \quad (2.15)$$

here,

$$q_w = -k_0 \left(\frac{\partial T}{\partial y} \right)_{y=0}, \quad (2.16)$$

Using Eq. (2.7) and Eq. (2.16) in Eq. (2.15) we get

$$(Re_x)^{-1/2} Nu_x = -\theta'(0). \quad (2.17)$$

2.2.3 Local Sherwood number

The ratio of the mass transfer by convection and diffusion mass transfer. It is a dimensionless parameter.

Defining it as,

$$Sh_x = \frac{x j_w}{D(C_w - C_\infty)}, \quad (2.18)$$

where,

$$j_w = -D \left(\frac{\partial C}{\partial y} \right)_{y=0}, \quad (2.19)$$

Using Eq. (2.7) and Eq. (2.19) in Eq. (2.18) we get

$$(Re_x)^{-1/2} Sh_x = -\phi'(0). \quad (2.20)$$

2.3 Numerical methodology

The system of equations Eq. (2.8) - Eq. (2.10) is solved through *bvp4c* method. In this problem, the initial guesses are precisely made to assure the convergent result. In this case, the values of parameters are selected in compliance with the convergence criteria. To implement the method, the system of equations Eq. (2.8) - Eq. (2.10) is converted to system of first order differential equations and solved along with boundary conditions.

The system of first order differential equations is:

$$\begin{aligned} \hat{y}_1 = f, & \quad \Rightarrow \hat{y}'_1 = f' = \hat{y}_2, \\ \hat{y}_2 = f', & \quad \Rightarrow \hat{y}'_2 = f'' = \hat{y}_3, \\ \hat{y}_3 = f'', & \quad \Rightarrow \hat{y}'_3 = f''' = \hat{y}_4, \\ \hat{y}_4 = f''', & \quad \Rightarrow \hat{y}'_4 = \frac{1}{\alpha_1 \hat{y}_1} [\hat{y}_4 + \alpha_1 (2\hat{y}_2 \hat{y}_4 - \hat{y}_3^2) - \hat{y}_2^2 + \hat{y}_1 \hat{y}_3 + \lambda(\hat{y}_5 - Nr \hat{y}_7)], \\ \hat{y}_5 = \theta, & \quad \Rightarrow \hat{y}'_5 = \theta' = \hat{y}_6, \\ \hat{y}_6 = \theta', & \quad \Rightarrow \hat{y}'_6 = \theta'' = -NbPr \hat{y}_6 \hat{y}_8 - PrNt \hat{y}_6^2 - Pr \hat{y}_1 \hat{y}_6, \\ \hat{y}_7 = \phi, & \quad \Rightarrow \hat{y}'_7 = \phi' = \hat{y}_8, \\ \hat{y}_8 = \phi', & \quad \Rightarrow \hat{y}'_8 = \phi'' = -Le \hat{y}_1 \hat{y}_8 - \frac{Nt}{Nb} \hat{y}'_6 + K_1 \hat{y}_7. \end{aligned} \quad (2.21)$$

The boundary conditions from Eq. (2.11) are transformed as

$$\begin{aligned} \hat{y}_1(0) = A, \quad \hat{y}_2(0) = 1, \quad \hat{y}_6(0) = -\gamma_1(\hat{y}_5(0) + 1), \quad \hat{y}_8(0) = -\gamma_1(\hat{y}_7(0) + 1), \\ \hat{y}_{inf}(2), \quad \hat{y}_{inf}(3), \quad \hat{y}_{inf}(5), \quad \hat{y}_{inf}(7). \end{aligned} \quad (2.22)$$

2.4 Discussion

We discuss the effect of different parameters on skin friction coefficient, local Sherwood number and local Nusselt number.

In Table 2.1, we see effect of different parameters on skin friction coefficient.

As Nr is increased, that is the higher buoyancy force restricts the fluid flow and thus the larger the skin friction coefficient. As α_1 which represents the second grade fluid parameter is increased, we obtain a large value of skin friction coefficient. When the value of λ is increased, the value of skin friction coefficient is decreased as the convection is enhanced by the fluid motion. When the value of Nb is increased, the skin friction coefficient is lowered because the elastic effects become significant thus opposing drag force is lowered. As the value of Nt is increased, the skin friction coefficient is increased. When the value of Le is increased it does not have a significant effect on skin friction coefficient.

In Table 2.2, we see the effect of different parameters on Local Nusselt Number.

As the value of Nr is increased, the heat transfer rate is enhanced. When the value of mixed convection parameter λ is increased, it does not effect the Nusselt number significantly. As Nb is increased, the heat transfer rate is enhanced. As Pr is increased, the heat transfer rate is lowered. When Nt is increased, the heat transfer rate is increased as Nt enhances the convection rate along the temperature gradient. When Le is increased, an decreasing trend in value of Nusselt number is noted.

In Table 2.3, we see the effect of different parameters on Sherwood number.

As we increase the value of Nr , a significant change in value of Sherwood number is not observed. When the value of Nb is increased, the decrease in mass transfer rate is observed. As the value of Pr is increased, the mass transfer rate is increased. As the value of Nt is increased, an increase in mass transfer rate is observed due to the increase in temperature gradient. As Le is increased, lower values for Sherwood number is observed as mass diffusivity is increased.

The graphs are constructed by considering $\alpha_1=0.2$, $\lambda=0.9$, $Nr=0.1$, $Pr=7$, $Le=2$, $A=0.1$.

Table 2.1: Influence of parameters on skin friction coefficient considering $Pr=7$, $A=0.1$, $\gamma_1=0.1$, $\gamma_2=0.1$.

Nr	α_1	λ	Nb	Nt	Le	$Re_x^{\frac{1}{2}}C_f(bvp4c)$
0.1	0.2	0.9	0.1	0.1	2	1.5956
0.4						1.6183
0.6						1.6336
0.1	0.1					1.3824
	0.3					1.7942
	0.4					1.9807
0.1	0.2	0.1				1.6052
		1.9				1.5836
		2.0				1.5824
0.1	0.2	0.9	0.3			1.5927
			0.5			1.5915
			0.7			1.5905
0.1	0.2	0.9	0.1	0.3		1.6011
				0.4		1.6038
				0.5		1.6066
0.1	0.2	0.9	0.1	0.1	1.9	1.5958
					2.1	1.5953
					2.2	1.5951

Fig. (2.1), depicts that $f'(\eta)$ velocity profile increases with the rise in value of α_1 . Fig. (2.2) elaborates that velocity profile $f'(\eta)$ rises with the enhancement in value of λ where $\lambda > 0$ shows assisting flow. Fig. (2.3) depicts that $f'(\eta)$ velocity profile lowers as the value of Nr is enhanced. Fig. (2.4) exhibits that $\theta(\eta)$ decays with the raise in the value of Nb . Fig. (2.5) elaborates that profile for temperature $\theta(\eta)$ rises with the enhancement in the value of Nt . Fig. (2.6) portrays that $\theta(\eta)$ lowers owing to the escalating values of Le . Fig. (2.7) depicts that $\theta(\eta)$ rises owing to the rise in value of Nr . Fig. (2.8) exhibits that the solute distribution $\phi(\eta)$ decays with the enhancement in the value of Nb . Fig. (2.9) portrays that the solute distribution $\phi(\eta)$ elevates with the rising values of Nt . Fig. (2.10) is drawn to see the impact on the solute distribution $\phi(\eta)$ with the enhanced value of Le . Fig. (2.11) portrays that the solute distribution $\phi(\eta)$ is enhanced with the increase in the value of Nr .

Table 2.2: Influence of parameters on local Nusselt number considering $\alpha_1=0.2$, $A=0.1$, $\gamma_1=0.1$, $\gamma_2=0.1$.

Nr	λ	Nb	Pr	Nt	Le	$Re_x^{-1/2} Nu_x(bvp4c)$
0.1	0.9	1	7	1.2	2	0.10723
0.5						0.10724
0.6						0.10725
0.1	0.2					0.10724
	0.9					0.10723
	1.2					0.10722
0.1	0.9	0.3				0.10615
		0.4				0.10628
		0.9				0.10705
0.1	0.9	1	2			0.11364
			4			0.10934
			6			0.10772
0.1	0.9	1	7	0.2		0.10554
				0.3		0.10567
				0.8		0.10645
0.1	0.9	1	7	1.2	1	0.10727
					1.2	0.10726
					1.5	0.10725

Table 2.3: Influence of parameters on local Sherwood number considering $\alpha_1=0.2$, $\lambda=0.9$, $A=0.5$, $\gamma_1=0.1$, $\gamma_2=0.1$.

Nr	Nb	Pr	Nt	Le	$Re_x^{-1/2} Sh_x(bvp4c)$
0.1	0.1	7	0.2	2	0.11403
0.8					0.11404
1.9					0.11406
0.1	0.3				0.10813
	0.5				0.10696
	0.6				0.10666
0.1	0.1	1			0.11149
		4			0.11341
		5			0.11367
0.1	0.1	7	0.1		0.10962
			0.4		0.12279
			0.6		0.13147
0.1	0.1	7	0.2	1.8	0.11489
				1.9	0.11444
				2.1	0.11363

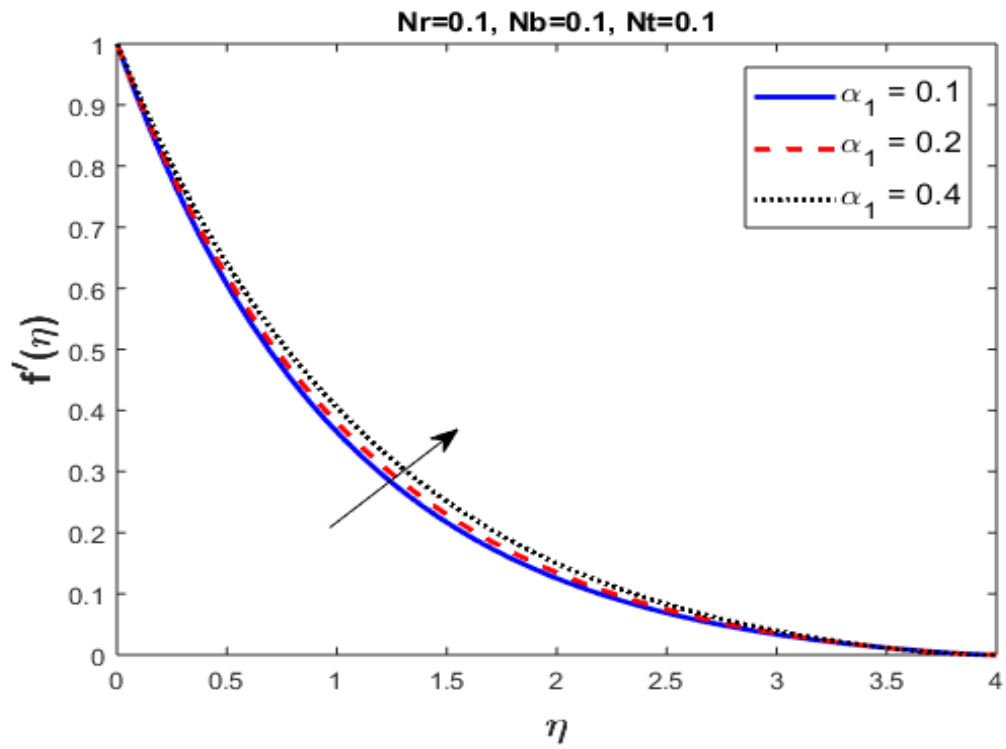


Figure 2.1: Computation of profile for velocity with respect to varied α_1 .

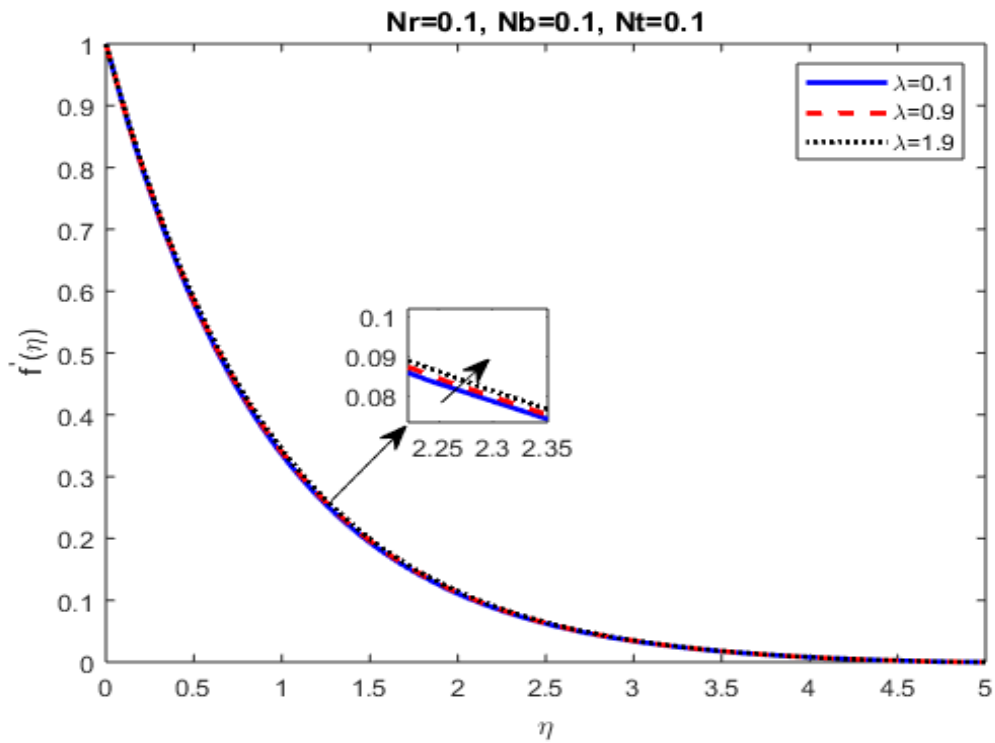


Figure 2.2: Computation of profile for velocity with respect to varied λ .

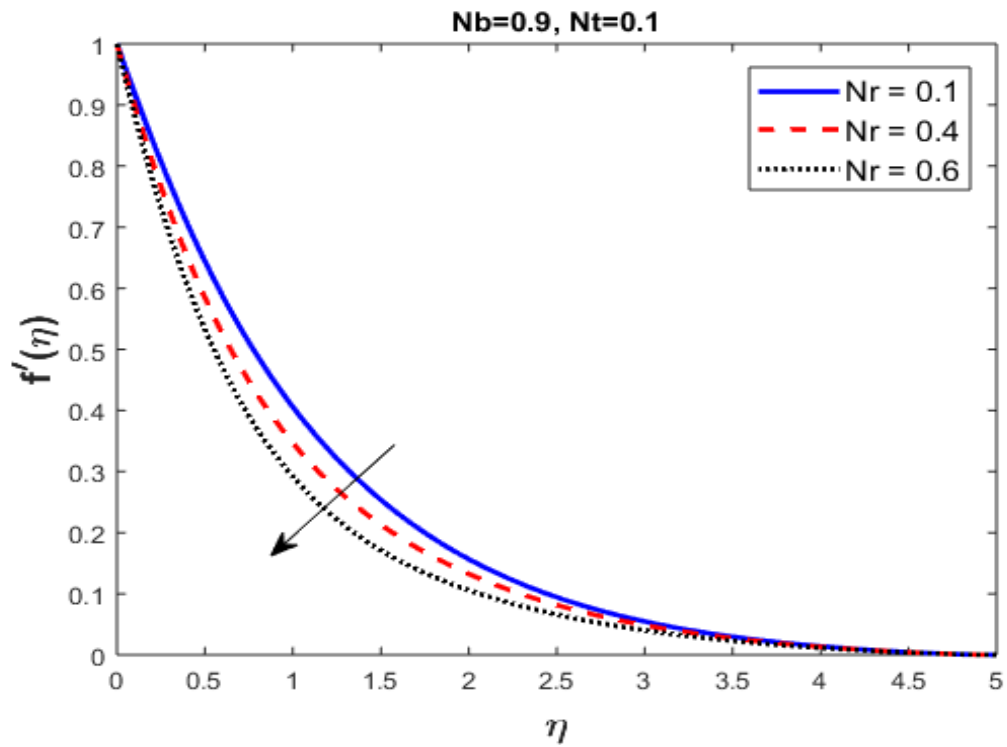


Figure 2.3: Computation of profile for velocity with respect to varied Nr .

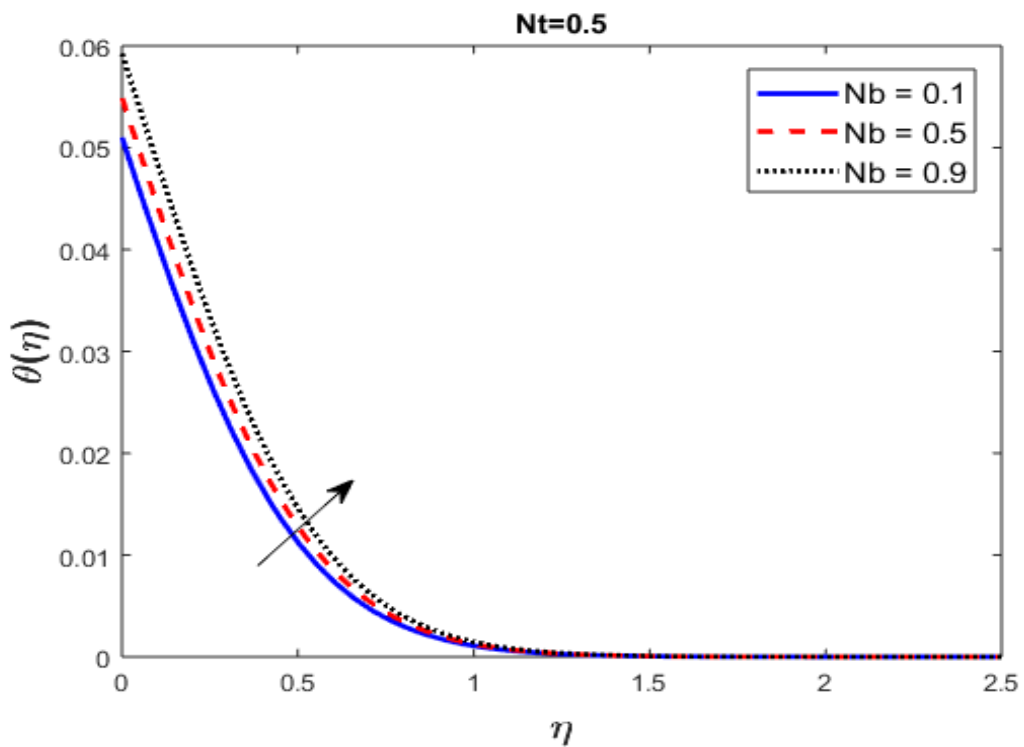


Figure 2.4: Computation of profile for temperature with respect to varied Nb .

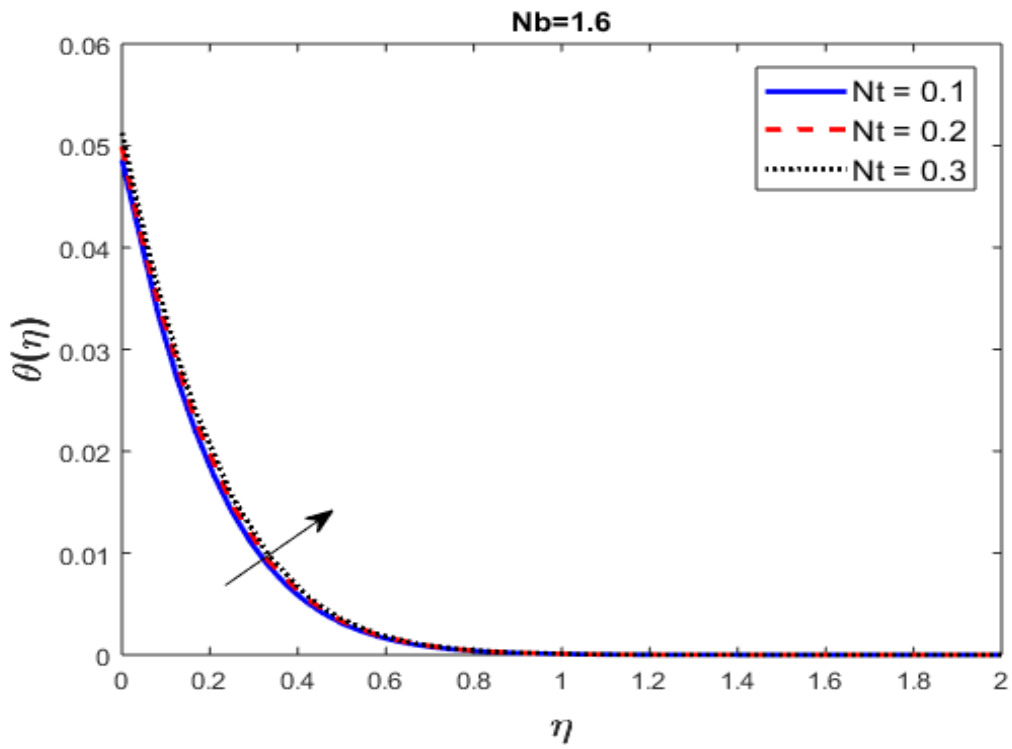


Figure 2.5: Computation of profile for temperature with respect to varied Nt .

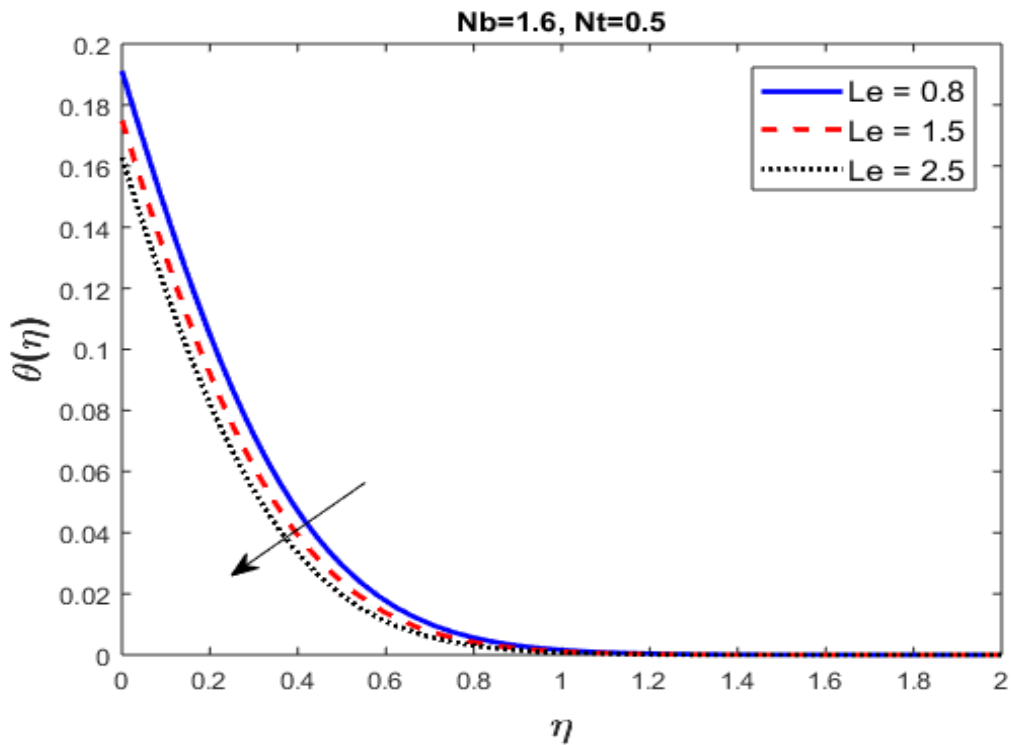


Figure 2.6: Computation of profile for temperature with respect to varied Le .

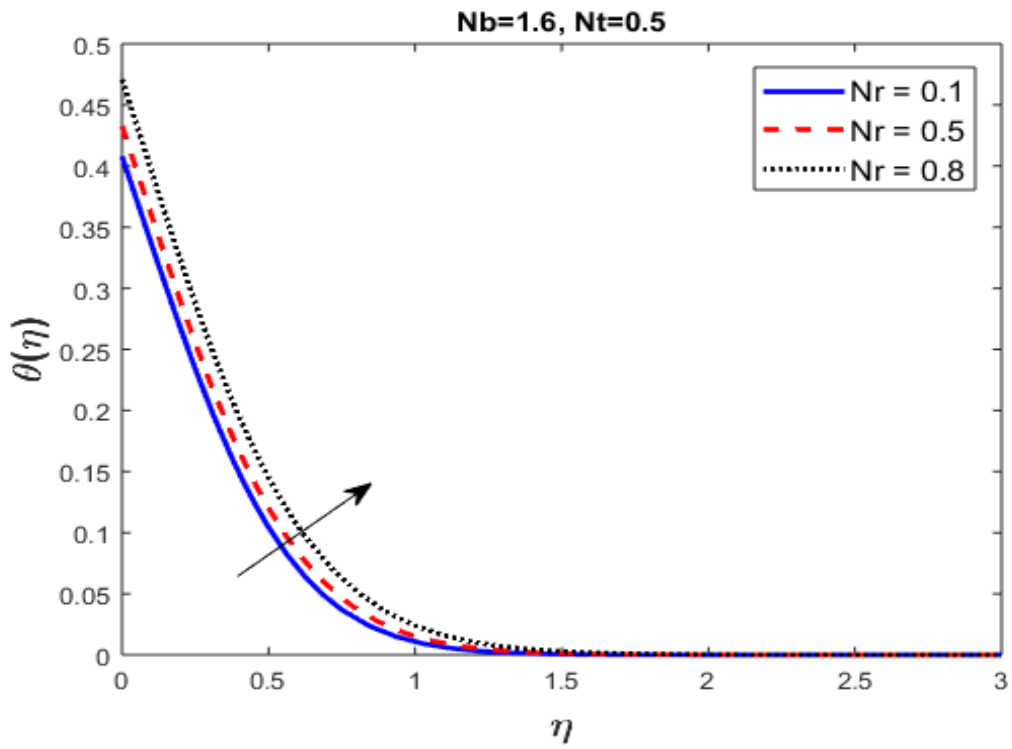


Figure 2.7: Computation of profile for temperature with respect to varied Nr .

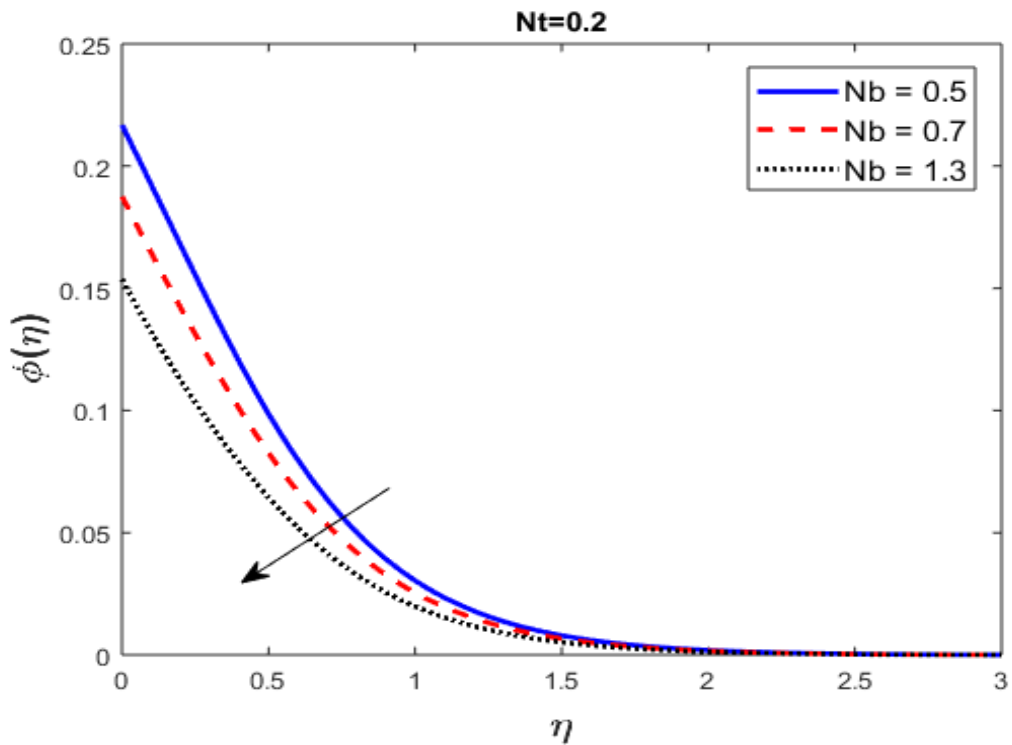


Figure 2.8: Computation of profile for concentration with respect to varied Nb .

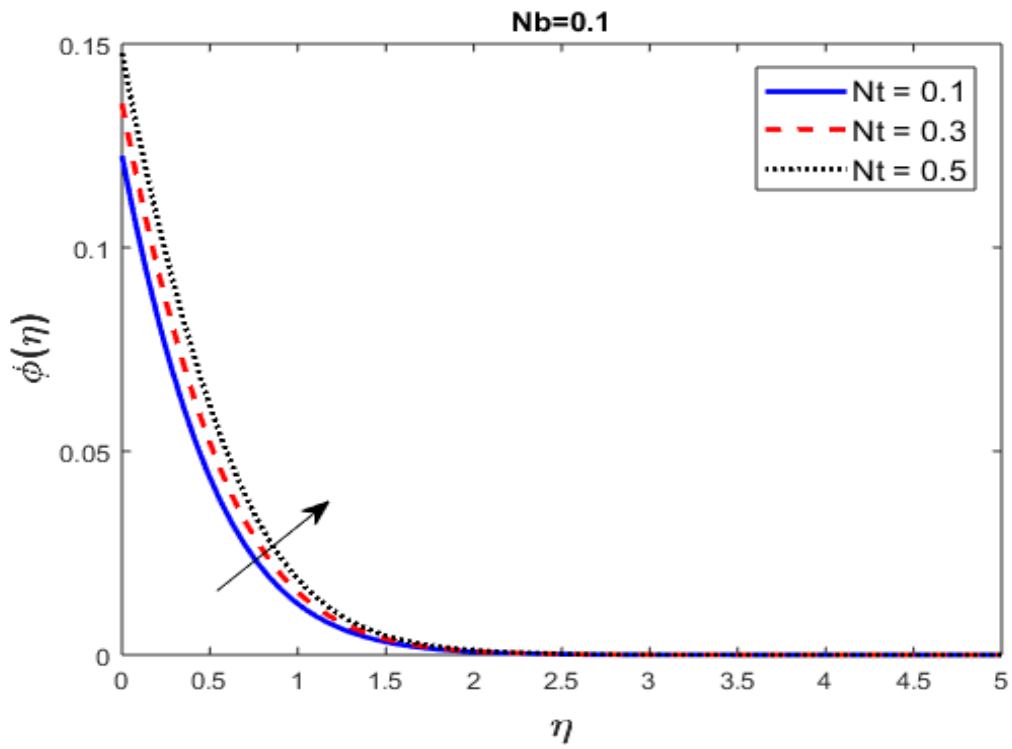


Figure 2.9: Computation of profile for concentration with respect to varied Nt .

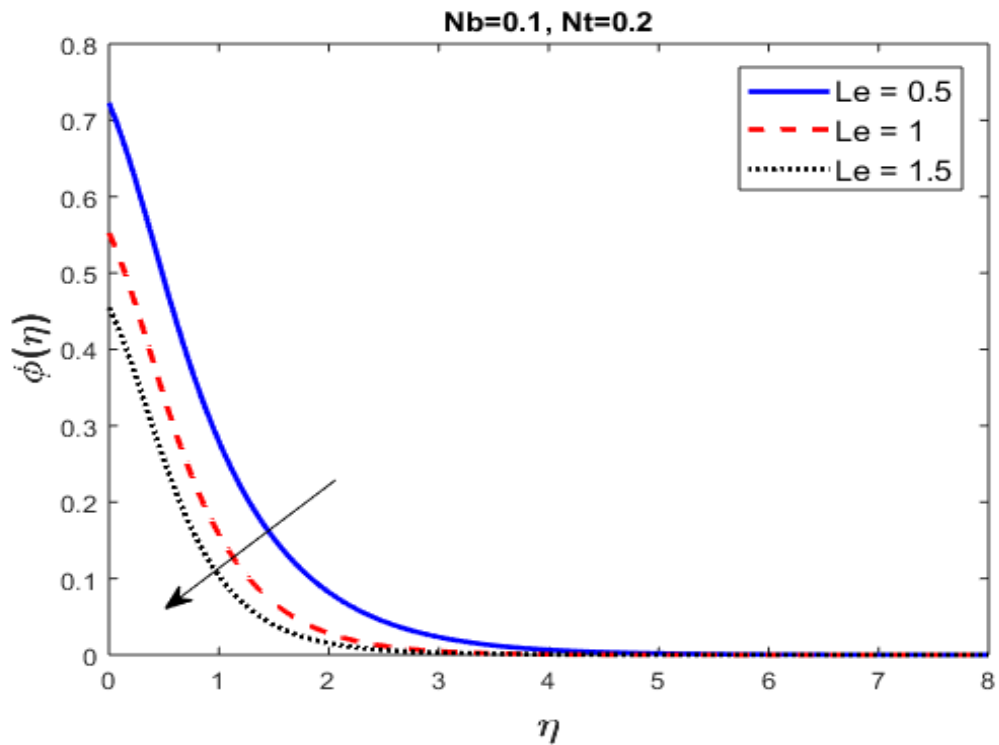


Figure 2.10: Computation of profile for concentration with respect to varied Le .

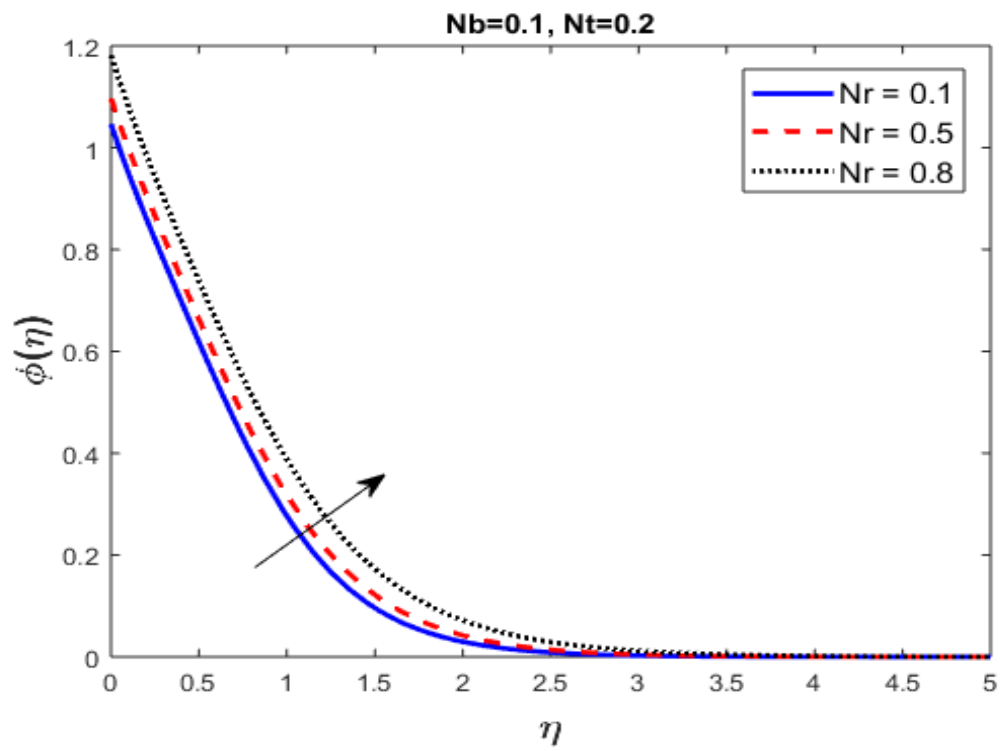


Figure 2.11: Computation of profile for concentration with respect to varied Nr .

Chapter 3

Impact of Arrhenius activation energy on bionanofluid MHD flow with variable thermal conductivity over nonlinearly stretching sheet

3.1 Introduction

In this chapter, we discuss the extension work that is motivated by Prasannakumara et al. [25] that explores the influence of Arrhenius activation energy and variable thermal conductivity on EMHD flow of bionanofluid over a nonlinear radiating stretching sheet in a porous medium is analyzed. A considered partial differential equations (PDEs) for the above model is written into a non-linear ordinary differential equations (ODEs) while applying similarity transformations. The resultant ODEs are solved by utilizing numerical methods such as *bvp4c*, shooting method and Galerkin method that is implemented in MATLAB. Graphs illustrate the effects of various relevant parameters and tables depict the influence of various parameters on local Nusselt number, skin friction coefficient, local Sherwood number and density of motile microorganisms.

3.2 Mathematical formulation

We consider the flow of bionanofluid over a nonlinear stretching sheet having MHD two-dimensional laminar steady flow with variable thermal conductivity, thermal radiation, Arrhenius activation energy and convective mass and heat boundary conditions. The surface

is assumed at $y = 0$. Normal to the direction of flow are applied variable magnetic field $B(x) = B_o x^{\frac{m-1}{2}}$ and variable electric field $E(x) = E_o x^{\frac{m-1}{2}}$. The sheet at $x - axis$ is being stretched with velocity $u_w = ax^m$ where $a, m > 0$ are positive constants. The induced magnetic field is assumed to be negligible as the magnetic Reynolds number is less than unity. The 2-D MHD boundary layer flow equations are given by [26]:

$$u_x + v_y = 0, \quad (3.1)$$

$$uu_x + vv_y = \nu u_{yy} - \frac{\sigma}{\rho_f} (B^2(x)u - E(x)B(x)) + \frac{1}{\rho_f} ((1 - C_\infty)\rho_{f\infty}\beta_T g^*(T - T_\infty) - (\rho_p - \rho_{p\infty})\beta_c g^*(C - C_\infty)) - \frac{\nu}{Kp^*}u, \quad (3.2)$$

$$uT_x + vT_y = \frac{1}{(\rho c_p)_f} (kT_y)_y - \frac{1}{(\rho c_p)_f} (q_r)_y + \frac{Q(x)}{(\rho c_p)_f} (T - T_\infty) + \frac{\sigma}{(\rho c_p)_f} (uB(x) - E(x))^2 + \frac{\mu}{(\rho c_p)_f} (u_y)^2 + \tau \left(D_B C_y T_y + \frac{D_T}{T_\infty} (T_y)^2 \right), \quad (3.3)$$

$$uC_x + vC_y = D_B C_{yy} + \frac{D_T}{T_\infty} T_{yy} - K_r^2 (C - C_\infty) \left(\frac{T}{T_\infty} \right)^n e^{\left(\frac{-E_a}{K_B T} \right)}, \quad (3.4)$$

$$uN_x + vN_y + \frac{bw_c}{(C_w - C_\infty)} N C_{yy} + \frac{bw_c}{(C_w - C_\infty)} N_y C_y = D_n N_{yy}. \quad (3.5)$$

where u represents the fluid movement component parallel to $x - axis$ and v represents fluid movement component parallel to $y - axis$, σ exhibits the electrical conductivity, ρ_f is bio-nanofluid's density, τ is the ratio of given heat capacity of nanoparticles versus the heat capacity of the given nanofluid, B denotes the magnetic field applied transverse to the direction of flow, g^* , β_t and β_c are respectively gravitational acceleration, volumetric thermal and solutal expansion coefficients. Here temperature is represented with T , the nanoparticles concentration is represented by C , N is the concentration of microorganisms, Kp^* is permeability of the porous medium, specific heat constant is represented by c_p , D_B represents Brownian diffusion, D_T and D_n are thermophoretic diffusion and diffusivity of microorganism respectively. q_r represents the heat flux through radiation, $Q(x)$ depicts the volumetric rate of heat generation and absorption. Kr is chemical reaction rate, n is fitted rate constant, E_a is activation energy, K_B is Boltzmann constant. Maximum swimming speed of cell is represented with w_c and b is chemotaxis constant.

The subjected boundary conditions are expressed as :

$$\begin{aligned}
y = 0 : \quad u = u_w = ax^m, \quad v = 0, \quad -k_0 \frac{\partial T}{\partial y} = h_1(T_w - T), \quad -D \frac{\partial C}{\partial y} = (C_w - C)h_2, \quad N = N_w, \\
y \rightarrow \infty : \quad u \rightarrow 0, \quad C \rightarrow C_\infty, \quad T \rightarrow T_\infty, \quad N \rightarrow N_\infty.
\end{aligned} \tag{3.6}$$

Here h_1 and h_2 are heat and mass transfer coefficients respectively. T_w is defined as the temperature of the fluid at the wall, C_w is defined as the concentration of nanoparticles in the fluid at the wall, N_w is defined as the motile microorganism density at the wall. T_∞ represents the temperature of the free stream, C_∞ gives the concentration of the free stream, N_∞ represents the motile microorganism density of the free stream.

The velocity components are defined as:

$$u = ax^m f'(\eta), \quad v = -\sqrt{\frac{\nu a(m+1)}{2}} x^{\frac{m-1}{2}} (f(\eta) + \eta \frac{m-1}{m+1} f'(\eta)), \tag{3.7}$$

The similarity variables are:

$$\eta = y \sqrt{\frac{a(m+1)}{2\nu}} x^{\frac{m-1}{2}}, \tag{3.8}$$

$$\theta(\eta) = \frac{T - T_\infty}{T_w - T_\infty}, \tag{3.9}$$

$$\phi(\eta) = \frac{C - C_\infty}{C_w - C_\infty}, \tag{3.10}$$

$$\chi(\eta) = \frac{N - N_\infty}{N_w - N_\infty}. \tag{3.11}$$

After applying the similarity transformation and using Eq. (3.7) - Eq. (3.11), the incompressibility condition Eq. (3.1) is trivially satisfied while Eq. (3.2) - Eq. (3.5) are reduced to:

$$f''' + ff'' - \frac{2m}{m+1} f'^2 - M(f' - E_1) + \lambda(\theta - Nr\phi) - Kpf' = 0, \tag{3.12}$$

$$(1 + \epsilon\theta + \frac{4}{3}Rd)\theta'' + \epsilon\theta'^2 + Pr_0(f\theta' + MEc(f' - E_1)^2 + Ec f''^2 + Nb\theta'\phi' + Nt\theta'^2 + s\theta) = 0, \tag{3.13}$$

$$\phi'' + \frac{Nt}{Nb}\theta'' + Sc(f\phi' - \frac{2}{m+1}\sigma_1\phi(1 + \delta\theta)^n e^{\frac{-E}{1+\delta\theta}}) = 0, \quad (3.14)$$

$$\chi'' + Sbf\chi' - Pe(\chi\phi'' + \chi'\phi') = 0, \quad (3.15)$$

From Prasad et al. [27] the thermal conductivity k is

$$k(T) = k_0(1 + \epsilon\theta), \quad (3.16)$$

The corresponding transformed boundary conditions are given as:

$$\begin{aligned} f(0) = 0, \quad f'(0) = 1, \quad \theta'(0) = -\beta_1(1 - \theta(0)), \quad \phi'(0) = -\beta_2(1 - \phi(0)), \quad \chi(0) = 1, \\ f'(\infty) = 0, \quad \theta(\infty) = 0, \quad \phi(\infty) = 0, \quad \chi(\infty) = 0. \end{aligned} \quad (3.17)$$

The resulting parameters are

$$\begin{aligned} M &= \frac{2\sigma B_0^2}{(m+1)\rho_f a}, \quad E_1 = \frac{E_0}{u_w B_0}, \quad K_p = \frac{2\nu x}{(m+1)u_w K p^*}, \\ G_r &= \frac{2g^*\beta_t(1 - C_\infty)\rho_{f\infty}(T_w - T_\infty)x^3}{\rho_f \nu^2(m+1)}, \quad Nr = \frac{(\rho_p - \rho_{f\infty})\beta_c(C_w - C_\infty)}{(1 - C_\infty)\rho_f \beta_t(T_w - T_\infty)}, \\ \lambda &= \frac{Gr}{Re_x^2}, \quad Pr_0 = \frac{\mu c_p}{k_0}, \quad Rd = \frac{4\sigma^* T_\infty^3}{k_0 k^*}, \quad s = \frac{2Qx}{(\rho C_p)_f u_w(m+1)}, \\ Ec &= \frac{u_w^2}{c_p(T_w - T_\infty)}, \quad Nb = \frac{\tau D_B(C_w - C_\infty)}{\nu}, \quad Nt = \frac{\tau D_T(T_w - T_\infty)}{\nu T_\infty}, \\ Sc &= \frac{\nu}{D_B}, \quad E = \frac{-Ea}{K_B T_\infty}, \quad \sigma_1 = \frac{Kr^2 x}{u_w}, \quad \delta = \frac{T_w - T_\infty}{T_\infty}, \\ \beta_1 &= \frac{h_1}{k_0} \sqrt{\frac{2\nu}{a(m+1)}} x^{\frac{-m+1}{2}}, \quad \beta_2 = \frac{h_2}{D} \sqrt{\frac{2\nu}{a(m+1)}} x^{\frac{-m+1}{2}}, \\ Sb &= \frac{\nu}{D_n}, \quad Pe = \frac{bw_c}{D_n}. \end{aligned}$$

Here, M denotes the magnetic parameter, E_1 is an electric parameter, K_p is the parameter for porosity, G_r represents the Grashof number, Nr represents the ratio of buoyancy parameter, mixed convection parameter is λ , Prandtl number is represented by Pr , Rd denotes the radiation parameter, local heat source parameter is depicted by s , Ec is the Eckert number,

parameter for Brownian motion is Nb , thermophoresis parameter is Nt , Sc denotes Schmidt number, E is activation parameter, σ_1 is chemical reaction parameter, δ is temperature difference, β_1 and β_2 are thermal and concentration Biot numbers respectively, Sb is bio convection Schmidt number and Pe is the Peclet number.

3.2.1 Skin friction coefficient

A key dimensionless parameter that determine the frictional drag on the surface is defined as skin friction coefficient C_f . It is described as

$$C_{fx} = \frac{\tau_w^*}{\rho u_w^2}, \quad (3.18)$$

here the wall shear stress is written as $\tau_w^* = \mu(\frac{\partial u}{\partial y})_{y=0}$. Thus we get

$$C_f \sqrt{Re_x} = \sqrt{\frac{m+1}{2}} f''(0), \quad (3.19)$$

where $Re_x = \frac{u_w x}{\nu}$ is known as the local Reynolds number.

3.2.2 Local Nusselt number

We measure local Nusselt number Nu_x at the surface to quantify the heat transfer at the wall.

$$Nu_x = \frac{xq_w}{k_0(T_w - T_\infty)}, \quad (3.20)$$

where $q_w = -k_0(\frac{\partial T}{\partial y})_{y=0}$. Thus we get

$$Re_x^{-\frac{1}{2}} Nu_x = -\sqrt{\frac{m+1}{2}} (1 + \frac{4Rd}{3}) \theta'(0). \quad (3.21)$$

3.2.3 Local Sherwood number

It is defined as

$$Sh_x = \frac{xj_w}{D(C_w - C_\infty)}, \quad (3.22)$$

where $j_w = -D(\frac{\partial C}{\partial y})_{y=0}$. We get

$$Re_x^{\frac{-1}{2}} Sh_x = -\sqrt{\frac{m+1}{2}} \phi'(0). \quad (3.23)$$

3.2.4 Local density of motile microorganisms

To define the motile microorganism's local density, we describe

$$Nn_x = \frac{xi_w}{D_n(N_w - N_\infty)}, \quad (3.24)$$

where $i_w = -D_n(\frac{\partial N}{\partial y})_{y=0}$. We get

$$Re_x^{\frac{-1}{2}} Nn_x = -\sqrt{\frac{m+1}{2}} \chi'(0). \quad (3.25)$$

3.3 Numerical Process

3.3.1 Linearization

To solve the system of ODEs with FEM, we make following transformation that is to transform the third order derivative into second order derivative. For details refer [28].

$$f' = F, \quad (3.26)$$

Thus the said system of equation will become as

$$F'' + fF' - \frac{2m}{m+1}F^2 - M(F - E_1) + \lambda(\theta - N_r\phi) - K_pF = 0, \quad (3.27)$$

$$\theta'' + \frac{\epsilon}{1 + \epsilon\theta + \frac{4}{3}Rd}\theta'^2 + \frac{Pr_0}{1 + \epsilon\theta + \frac{4}{3}Rd} (f\theta' + ME_c(F - E_1)^2 + E_cF'^2 + N_b\theta'\phi' + N_t\theta'^2 + s\theta) = 0, \quad (3.28)$$

$$\phi'' + \frac{N_t}{N_b}\theta'' + Sc \left(f\phi' - \frac{2}{m+1}\sigma_1\phi(1 + \delta\theta)^n e^{\frac{-E}{1+\delta\theta}} \right) = 0, \quad (3.29)$$

$$\chi'' + S_b f \chi - P_e(\chi\phi'' + \chi'\phi') = 0. \quad (3.30)$$

The corresponding boundary conditions will become

$$\begin{aligned} \eta = 0 : \quad & f = 0, \quad F = 1, \quad \theta' = -(1 - \theta)\beta_1, \quad \phi' = -(1 - \phi)\beta_2, \quad \chi = 1, \\ \eta \rightarrow \infty : \quad & F = 0, \quad \theta = 0, \quad \phi = 0, \quad \chi = 0. \end{aligned} \quad (3.31)$$

The above equations are non-linear and coupled. We will use Taylor series to linearize them. We start with Eq. (3.27).

$$F'' = -fF' + \frac{2m}{m+1}F^2 + M(F - E_1) - \lambda(\theta - N_r\phi) + K_pF,$$

In the above equation, we define $h(\eta, F, F')$ as

$$h(\eta, F, F') = -fF' + \frac{2m}{m+1}F^2 + M(F - E_1) - \lambda(\theta - N_r\phi) + K_pF,$$

Now we define,

$$A_n = - \left(\frac{\partial h}{\partial F'} \right)_n = -[-f_n] = f_n,$$

Thus,

$$A_n = f_n,$$

And,

$$\begin{aligned} B_n &= - \left(\frac{\partial h}{\partial F} \right)_n = - \left[\frac{4m}{m+1}F_n + M + K_p \right], \\ B_n &= - \frac{4m}{m+1}F_n - M - K_p, \end{aligned}$$

Now,

$$\begin{aligned} D_n &= h(\eta, F_n, F'_n) - \left(\frac{\partial h}{\partial F} \right)_n F_n - \left(\frac{\partial h}{\partial F'} \right)_n F'_n, \\ D_n &= h(\eta, F_n, F'_n) + B_n F_n + A_n F'_n, \end{aligned}$$

where $h(\eta, F_n, F'_n)$, A_n and B_n are defined above. Hence, the linearized equation for F is given as

$$F''_{n+1} + A_n(\eta, F_n, F'_n)F'_{n+1} + B_n(\eta, F_n, F'_n)F_{n+1} = D_n(\eta, F_n, F'_n),$$

Similarly, for other equations Eq. (3.28), Eq. (3.29) and Eq. (3.30) same procedure as above is used to obtain the system of linear equation along with boundary conditions.

3.3.2 Finite element method

The system of ODE's is linearized using Taylor series and we get the following system that will be solved iteratively.

$$f' = F, \tag{3.32}$$

$$F''_{n+1} + A_n(\eta, F_n, F'_n)F'_{n+1} + B_n(\eta, F_n, F'_n)F_{n+1} = D_n(\eta, F_n, F'_n), \tag{3.33}$$

$$\theta''_{n+1} + A_n(\eta, \theta_n, \theta'_n)\theta'_{n+1} + B_n(\eta, \theta_n, \theta'_n)\theta_{n+1} = D_n(\eta, \theta_n, \theta'_n), \tag{3.34}$$

$$\phi''_{n+1} + A_n(\eta, \phi_n, \phi'_n)\phi'_{n+1} + B_n(\eta, \phi_n, \phi'_n)\phi_{n+1} = D_n(\eta, \phi_n, \phi'_n), \tag{3.35}$$

$$\chi''_{n+1} + A_n\chi'_{n+1}(\eta, \chi_n, \chi'_n) + B_n(\eta, \chi_n, \chi'_n)\chi_{n+1} = D_n(\eta, \chi_n, \chi'_n), \tag{3.36}$$

Along with the boundary conditions

$$\begin{aligned} \eta = 0 : \quad & f = 0, \quad F = 1, \quad \theta' = -\beta_1(1 - \theta), \quad \phi' = -\beta_2(1 - \phi), \quad \chi = 1, \\ \eta \rightarrow \infty : \quad & F = 0, \quad \phi = 0, \quad \theta = 0, \quad \chi = 0. \end{aligned} \tag{3.37}$$

Finite element method at first will be used for Eq. (3.33). For simplicity we write it as follows:

$$F''_{n+1} + A_n F'_{n+1} + B_n F_{n+1} = D_n, \tag{3.38}$$

Multiplying the Eq. (3.38) to a weight function $w(\eta)$ and integrating over the domain $[a, b]$, we get

$$\int_a^b \left(\frac{d^2 F_{n+1}}{d\eta^2} + A_n \frac{dF_{n+1}}{d\eta} + B_n F_{n+1} \right) w(\eta) d\eta = \int_a^b D_n w(\eta) d\eta,$$

$$\int_a^b \frac{d^2 F_{n+1}}{d\eta^2} w(\eta) d\eta + \int_a^b A_n \frac{dF_{n+1}}{d\eta} w(\eta) d\eta + \int_a^b B_n F_{n+1} w(\eta) d\eta = \int_a^b D_n w(\eta) d\eta,$$

Integrate the left hand side by parts. For Dirichlet boundary conditions, weight function $w(\eta)$ is chosen in such a way that it has zero value at the boundary that is $w(a)=w(b)=0$. Therefore, above equation will become

$$-\int_a^b \frac{dF_{n+1}}{d\eta} \frac{dw}{d\eta} d\eta + \int_a^b A_n \frac{dF_{n+1}}{d\eta} w(\eta) d\eta + \int_a^b B_n F_{n+1} w(\eta) d\eta = \int_a^b D_n w(\eta) d\eta, \quad (3.39)$$

The above Eq. (3.39) is a weak formulation. Let the solution be of the form

$$F_{n+1} = \sum_{i=1}^{Ne} \phi_i (F_{n+1})_i,$$

where ϕ_i are the basis function and Ne are total number of nodes in an element.

Here, we use **Galerkin method** that requires the basis function to be defined same as above. Furthermore, if $[\eta_i, \eta_{i+1}]$ are nodes of finite element, then Eq. (3.39) will become

$$\begin{aligned} & -\sum_{i=1}^{Ne} \left[\int_{\eta_i}^{\eta_{i+1}} \frac{d\phi_i}{d\eta} \frac{d\phi_j}{d\eta} d\eta \right] (F_{n+1})_i + \sum_{i=1}^{Ne} \left[\int_{\eta_i}^{\eta_{i+1}} A_n \frac{d\phi_i}{d\eta} \phi_j d\eta \right] (F_{n+1})_i \\ & + \sum_{i=1}^{Ne} \left[\int_{\eta_i}^{\eta_{i+1}} B_n \phi_i \phi_j d\eta \right] (F_{n+1})_i = \int_{\eta_i}^{\eta_{i+1}} D_n \phi_j d\eta, \end{aligned}$$

$$\sum_{i=1}^{Ne} \left[-\int_{\eta_i}^{\eta_{i+1}} \frac{d\phi_i}{d\eta} \frac{d\phi_j}{d\eta} d\eta + \int_{\eta_i}^{\eta_{i+1}} A_n \frac{d\phi_i}{d\eta} \phi_j d\eta + \int_{\eta_i}^{\eta_{i+1}} B_n \phi_i \phi_j d\eta \right] (F_{n+1})_i = \int_{\eta_i}^{\eta_{i+1}} D_n \phi_j d\eta, \quad (3.40)$$

Defining the following notations:

$$L_{ij} = -\int_{\eta_i}^{\eta_{i+1}} \frac{d\phi_i}{d\eta} \frac{d\phi_j}{d\eta} d\eta,$$

$$C_{ij} = \int_{\eta_i}^{\eta_{i+1}} A_n \frac{d\phi_i}{d\eta} \phi_j d\eta,$$

$$M_{ij} = \int_{\eta_i}^{\eta_{i+1}} B_n \phi_i \phi_j d\eta,$$

$$R_j = \int_{\eta_i}^{\eta_{i+1}} D_n \phi_j d\eta,$$

where,

$$K_{ij} = L_{ij} + C_{ij} + M_{ij},$$

Thus Eq. (3.40) becomes

$$\sum_{i=1}^{Ne} K_{ij} (F_{n+1})_i = R_j,$$

For a single element the matrix will be as follows and called as element stiffness matrix.

$$\begin{bmatrix} K_{11} & K_{12} \\ K_{21} & K_{22} \end{bmatrix} \begin{bmatrix} F_1 \\ F_2 \end{bmatrix}^{n+1} = \begin{bmatrix} R_1 \\ R_2 \end{bmatrix}$$

The global stiffness matrix will be defined as below:

$$\begin{bmatrix} K_{11} & K_{12} & 0 & \cdots & 0 \\ K_{21} & K_{22} & K_{23} & \cdots & 0 \\ 0 & K_{32} & K_{33} & \cdots & 0 \\ \vdots & \vdots & \vdots & \ddots & \vdots \\ 0 & 0 & 0 & \cdots & K_{NN} \end{bmatrix} \begin{bmatrix} F_1 \\ F_2 \\ F_3 \\ \vdots \\ F_N \end{bmatrix}^{n+1} = \begin{bmatrix} R_1 \\ R_2 + R_3 \\ R_3 + R_4 \\ \vdots \\ R_N \end{bmatrix} \quad (3.41)$$

Similarly, for other remaining equations we observe the same above procedure and solve them by using MATLAB.

3.3.3 Shooting method

In shooting method, a boundary value problem is transformed into an initial value problem. It is then reduced to a system of first order ODEs. To apply the method an initial guess is chosen. Then initial value problem is solved by using numerical method like Runge-Kutta method of order 5. For further details refer [29]. To transform the non-linear ODEs into system of first order differential equations we define as

$$\begin{aligned}
y_1 &= f, & y_2 &= f', & y_3 &= f'', \\
y_4 &= \theta, & y_5 &= \theta', \\
y_6 &= \phi, & y_7 &= \phi', \\
y_8 &= \chi, & y_9 &= \chi'.
\end{aligned} \tag{3.42}$$

Using (3.42) we get the following system of first order differential equations,

$$\begin{aligned}
y_1' &= y_2, \\
y_2' &= y_3, \\
yy1 &= y_3' = -y_1y_3 + \frac{2m}{m+1}y_2^2 + M(y_2 - E_1) - \lambda(\theta - N_r\phi) + Kpy_2, \\
y_4' &= y_5, \\
yy2 &= y_5' = -\epsilon y_5^2 - \frac{Pr_0}{(1 + \epsilon\theta + \frac{4}{3})Rd} (y_1y_5 + MEc(y_2 - E_1)^2 + Ecy_3^2 + Nby_5y_7 + Nty_5^2 + sy_4), \\
y_6' &= y_7, \\
yy3 &= y_7' = -\frac{Nt}{Nb}y_5' - Sc \left(y_1y_7 - \frac{2m}{m+1}\sigma_1\phi(1 + \delta\theta)^n e^{\frac{-E}{1+\delta\theta}} \right), \\
y_8' &= y_9, \\
yy4 &= y_9' = -Sby_1y_9 + Pe(y_8y_7' + y_7y_9).
\end{aligned} \tag{3.43}$$

The boundary conditions (3.17) are transformed into initial boundary conditions as

$$\begin{aligned}
f(0) &= 0, & f'(0) &= 1, & f''(0) &= \lambda_1, & \theta(0) &= \frac{\lambda_2 + \beta_1}{\beta_1}, & \theta'(0) &= \lambda_2, \\
\phi(0) &= \frac{\lambda_3 + \beta_2}{\beta_2}, & \phi'(0) &= \lambda_3, & \chi(0) &= 1, & \chi'(0) &= \lambda_4.
\end{aligned} \tag{3.44}$$

where λ_1 , λ_2 , λ_3 and λ_4 are initial guesses.

Then we solve using MATLAB.

3.3.4 bvp4c

In this problem, we use MATLAB *bvp4c* solver. Obtained results through shooting method and Galerkin method are verified using *bvp4c* method. Initial mesh points are given by initial guess

to get the required accuracy. For more details see [30].

To apply *bvp4c* method, we consider the system of first order differential equations defined in (3.43). The corresponding boundary conditions are

$$\begin{aligned} y_1(0) = 0, \quad y_2(0) = 1, \quad y_5(0) = \beta_1(y_4(0) - 1), \quad y_7(0) = \beta_2(y_6(0) - 1), \quad y_8(0) = 1, \\ y_{inf}(2) = 0, \quad y_{inf}(4) = 0, \quad y_{inf}(6) = 0, \quad y_{inf}(8) = 0. \end{aligned} \quad (3.45)$$

3.4 Discussion

Table 3.1: Comparison of $-\theta'(0)$ for various values of Pr_0 .

Pr_0	Goyal and Bhargava [31]	Sidawi and Gorla [32]	Current Results	
			(bvp4c)	(FEM)
0.07	0.0698	0.0656	0.0656	0.0698
0.20	0.1691	0.1691	0.1691	0.1691
0.70	0.4539	0.5349	0.4539	0.4540
2.00	0.9113	0.9114	0.9114	0.9114
7.00	1.8954	1.8954	1.8954	1.8955
20.00	3.3539	3.3539	3.3539	3.3540
70.00	6.4621	6.4622	6.4623	6.4621

In Table 3.1, a comparison is drawn for the case of $-\theta'(0)$ for different values of Pr_0 with published results. An excellent agreement between the published and present results are achieved.

In Table 3.2, we discuss the impact of different parameters on skin friction coefficient.

For Table 3.2, the M indicates a magnetic parameter. It represents the Lorentz force applied normally that opposes the flow of fluid. As M is enhanced, the value of skin friction coefficient is enlarged.

The parameter λ is a mixed convection parameter. With the enhancement in λ the skin friction coefficient decreases.

The parameter Nr represents the ratio of buoyancy parameter. Physically, as we increase the value of Nr, the stronger buoyancy force acting normally supports the vertical flow of nanofluid. Therefore, the value of skin friction coefficient is increased.

The Kp indicates the porosity parameter. As we increase the value of Kp the velocity of nanofluid decreases thus the value of skin friction coefficient increases.

Table 3.2: Effect of different parameters on skin friction coefficient
 considering $m=1$, $E_1=0$, $\epsilon=0.1$, $Sc=1$, $E=0.5$, $\delta=0.3$, $\sigma_1=0.3$, $n=0.5$, $Sb=0.5$, $Pe=0.5$, $\beta_1=0.4$,
 $\beta_2=0.4$.

M	λ	Nr	Kp	Rd	Pr	Ec	Nb	Nt	s	bvp4c	SM	FEM	Abs.Diff
													(bvp4c-FEM)
0.2										1.2480	1.2480	1.2508	2.8000e-03
0.5										1.3462	1.3461	1.3487	2.5000e-03
0.7										1.4074	1.4074	1.4102	2.8000e-03
0.3	0.3									1.2535	1.2533	1.2574	3.9000e-03
	0.5									1.1996	1.1991	1.1999	3.0000e-04
	0.7									1.1486	1.1481	1.1490	4.0000e-04
0.3	0.2	0.4								1.2852	1.2850	1.2885	3.3000e-03
		0.5								1.2887	1.2884	1.2927	4.0000e-03
		0.8								1.2989	1.2987	1.3053	6.4000e-03
0.3	0.2	0.3	0.6							1.3169	1.3167	1.3194	2.5000e-03
			0.7							1.3513	1.3511	1.3537	2.4000e-03
			0.9							1.4175	1.4173	1.4197	2.2000e-03
0.3	0.2	0.3	0.5	0.4						1.2812	1.2810	1.2838	2.6000e-03
				0.5						1.2807	1.2805	1.2832	2.5000e-03
				0.7						1.2795	1.2793	1.2820	2.5000e-03
0.3	0.2	0.3	0.5	0.3	6.2					1.2811	1.2809	1.2837	2.6000e-03
					7					1.2818	1.2816	1.2844	2.6000e-03
					7.5					1.2821	1.2819	1.2848	2.7000e-03
0.3	0.2	0.3	0.5	0.3	6.8	0.5				1.2486	1.2485	1.2508	2.2000e-03
						0.6				1.2329	1.2326	1.2348	1.9000e-03
						0.9				1.1871	1.1869	1.1891	2.0000e-03
0.3	0.2	0.3	0.5	0.3	6.8	0.3	0.4			1.2782	1.2780	1.2808	2.6000e-03
							0.5			1.2747	1.2745	1.2774	2.7000e-03
							0.8			1.2634	1.2633	1.2663	2.9000e-03
0.3	0.2	0.3	0.5	0.3	6.8	0.3	0.3	0.2		1.2781	1.2780	1.2812	3.1000e-03
								0.3		1.2734	1.2736	1.2774	4.0000e-03
								0.4		1.2681	1.2683	1.2729	4.8000e-03
0.3	0.2	0.3	0.5	0.3	6.8	0.3	0.3	0.1	0.1	1.2817	1.2817	1.2843	2.6000e-03
									0.15	1.2735	1.2736	1.2762	2.7000e-03
									0.2	1.2632	1.2629	1.2659	2.7000e-03

The parameter Rd represents the radiation parameter. As we increase the radiation parameter, the negligible effects are observed on the skin friction coefficient. The parameter Pr represents the Prandtl number. Increasing Prandtl number has negligible effects on the skin friction coefficients. The parameter Ec is the Eckert number. As we increase the Eckert number the skin friction coefficient decreases. The parameter Nt represents the thermophoresis parameter.

They have negligible effect on flow velocity and consequently on the coefficient of skin friction.

The s represents the local heat source/sink parameter. As we increase the value of s we observe an increase in the flow velocity and thus it overcomes the resistance. Therefore, the value of the skin friction coefficient decreases.

Table 3.3: Effect of different parameters on local Nusselt number considering $m=1$, $\epsilon=0.2$, $s=0.1$, $Sc=1$, $E=0.5$, $\sigma_1=\delta=0.3$, $n=0.5$, $Sb=0.5$, $Pe=0.5$, $Nb=0.3$, $\beta_1=0.4$, $\beta_2=0.4$.

M	E_1	λ	Nr	Kp	Rd	Pr	Ec	Nt	bvp4c	SM	FEM	Abs.Diff
												(bvp4c-FEM)
0.2									0.1166	0.1164	0.1188	2.2e-03
0.5									0.0395	0.0393	0.0429	3.4e-03
0.6									0.0148	0.0145	0.0154	6.0e-04
0.3	0								0.0904	0.0902	0.0930	2.6e-03
	0.1								0.1164	0.1163	0.1130	3.4e-03
	0.2								0.1373	0.1371	0.1332	4.1e-03
0.3	0	0.3							0.0977	0.0975	0.0995	1.8e-03
		0.5							0.1184	0.1184	0.1112	7.2e-03
		0.7							0.1314	0.1312	0.1310	4.0e-04
0.3	0	0.2	0.4						0.0887	0.0885	0.0888	1.0e-04
			0.5						0.0869	0.0866	0.0886	1.7e-03
			0.8						0.0816	0.0816	0.0818	2.0e-04
0.3	0	0.2	0.3	0.6					0.0791	0.0789	0.0785	6.0e-04
				0.7					0.0679	0.0678	0.0678	1.0e-04
				0.8					0.0568	0.0568	0.0569	1.0e-04
0.3	0	0.2	0.3	0.5	0.4				0.1063	0.1062	0.1088	2.5e-03
					0.5				0.1223	0.1220	0.1247	2.4e-03
					0.7				0.1542	0.1540	0.1563	2.1e-03
0.3	0	0.2	0.3	0.5	0.3	2			0.1318	0.1321	0.1310	8.0e-04
						5			0.1118	0.1118	0.1133	1.5e-03
						7.5			0.0819	0.0819	0.0829	1.0e-03
0.3	0	0.2	0.3	0.5	0.3	6.8	0.1		0.2909	0.2909	0.2928	1.9e-03
							0.2		0.1883	0.1882	0.1905	2.2e-03
							0.3		0.0904	0.0901	0.0903	1.0e-04
0.3	0	0.2	0.3	0.5	0.3	6.8	0.3	0.2	0.0709	0.0709	0.0710	1.0e-04
								0.3	0.0503	0.0500	0.0511	8.0e-04
								0.4	0.0283	0.0280	0.0289	6.0e-04

In Table 3.3, we discuss the influence of various parameters on local Nusselt number.

The m represents a positive constant. As the value of m is increased, we observe a decrease in the value of local Nusselt number.

The increase in magnetic field parameter M hinders the motion of the fluid which result into lowering of heat transfer rate.

The E_1 represents the electric field parameter. The increase in electric parameter results in increase of Nusselt number. The temperature difference between the surface and upper layers increases and thus the rate at which heat is transferred increases.

The λ represents the mixed convection parameter. The increase in value of λ causes Nu_x to increase. Mixed convection aids the flow of fluid in order to transfer heat.

The Nr represents the ratio of buoyancy parameter. It has negligible effect on heat transfer rate. The increase in porosity parameter K_p decreases the heat transfer rate. The heat transfer rate reduces when fluid attracts to pores structured medium.

The radiation parameter is represented by Rd . The increase in Rd results in increase of heat transfer rate. The radiation is absorbed by the particles of the system and thus creating a temperature difference between surface and upper layers. Therefore, the heat is transferred at a higher rate.

The Eckert number is represented by Ec . An increase in Ec resulted in decrease of heat transfer rate. The Ec is the relationship between a flow's kinetic energy and boundary layer enthalpy difference and characterizes the heat transfer dissipation. So as we increase Ec it lowers the heat transfer rate.

The thermophoresis is represented by Nt . The increase in the value of Nt resulted into decrease of Nusselt number. The increase in Pr results in decrease of heat transfer rate.

In Table 3.4, we discuss the effect of different parameters on local Sherwood number. As m increases the Sherwood number increases. For the parameters E_1 , K_p , Rd , Ec , Nb and n the Sherwood number has negligible change in its values. For Sc the Sherwood number decreases. For σ_1 , E and δ there is negligible change in the Sherwood number.

Table 3.4: Effect of different parameters on local Sherwood number considering $m=1$, $M=0.3$, $\lambda=0.2$, $Nr=0.3$, $\epsilon=0.2$, $Nt=0.1$, $Pr=6.8$, $s=0.1$, $Sb=0.5$, $Pe=0.5$, $\beta_1=0.4$, $\beta_2=0.4$.

E_1	Kp	Rd	Ec	Nb	Sc	σ_1	E	δ	n	bvp4c	SM	FEM	Abs.Diff
													(bvp4c-FEM)
0.3										0.2855	0.2856	0.2643	2.12e-02
0.5										0.2864	0.2864	0.2656	2.08e-02
0.7										0.2863	0.2861	0.2677	1.86e-02
0.5	0.6									0.2858	0.2858	0.2665	1.93e-02
	0.7									0.2860	0.2859	0.2675	1.85e-02
	0.9									0.2864	0.2864	0.2695	1.69e-02
0.5	0.5	0.4								0.2849	0.2849	0.2649	2.00e-02
		0.5								0.2844	0.2844	0.2644	2.00e-02
		0.7								0.2836	0.2835	0.2635	2.01e-02
0.5	0.5	0.3	0.2							0.2817	0.2817	0.2598	2.19e-02
			0.3							0.2856	0.2855	0.2656	2.00e-02
			0.5							0.2925	0.2925	0.2752	1.73e-02
0.5	0.5	0.3	0.3	1.3						0.2856	0.2855	0.2657	1.99e-02
				1.7						0.2859	0.2859	0.2664	1.95e-02
				2						0.2862	0.2862	0.2671	1.91e-02
0.5	0.5	0.3	0.3	1	1					0.2649	0.2648	0.2435	2.14e-02
					1.3					0.2785	0.2785	0.2580	2.05e-02
					1.5					0.2856	0.2855	0.2656	2.00e-02
0.5	0.5	0.3	0.3	1	1.5	0.5				0.2939	0.2939	0.2800	1.39e-02
						0.6				0.2975	0.2975	0.2855	1.20e-02
						0.9				0.3061	0.3066	0.2980	8.10e-03
0.5	0.5	0.3	0.3	1	1.5	0.3	1			0.2833	0.2832	0.2562	2.71e-02
							1.3			0.2803	0.2802	0.2414	3.89e-02
							1.5			0.2785	0.2785	0.2310	4.75e-02
0.5	0.5	0.3	0.3	1	1.5	0.3	0.8	0.4		0.2867	0.2867	0.2683	1.84e-02
								0.6		0.2889	0.2889	0.2732	1.57e-02
								1		0.2931	0.2933	0.2817	1.14e-02
0.5	0.5	0.3	0.3	1	1.5	0.3	0.8	0.3	0.8	0.2851	0.2851	0.2647	2.04e-02
									1	0.2856	0.2855	0.2656	2.00e-02
									1.5	0.2867	0.2867	0.2678	1.89e-02

In Table 3.5, we discuss the effect of different parameters on motile microorganisms. As the value of m increases the motile microorganisms increases. There is no change in the values of motile microorganisms when the parameter Nb , Sc , E , δ and n increases. With the increase of Nt , Sb and Pe the density of microorganisms increases.

The following graphs are constructed by considering $m = 1$, $M = 0.3$, $Rd = 0.3$, $\delta = 0.3$,

Table 3.5: Effect of different parameters on density for motile microorganisms considering $m=1$, $M=0.3$, $E_1=0$, $\lambda=0.2$, $Nr=0.3$, $Kp=0.5$, $Rd=0.3$, $\epsilon=0.2$, $Pr=6.8$, $\sigma_1=0.3$, $Ec=0.3$, $\delta=0.3$, $s=0.1$, $\beta_1=\beta_2=0.4$.

Nb	Nt	Sc	E	δ	n	Sb	Pe	bvp4c	SM	FEM	Abs.Diff (bvp4c-FEM)
0.4								0.6498	0.6495	0.6389	1.09e-02
0.5								0.6478	0.6475	0.6370	1.08e-02
0.8								0.6462	0.6460	0.6354	1.08e-02
0.3	0.1							0.6537	0.6537	0.6428	1.09e-02
	0.2							0.6790	0.6787	0.6683	1.07e-02
	0.3							0.7076	0.7076	0.6971	1.05e-02
0.3	0.1	1.3						0.6608	0.6605	0.6504	1.04e-02
		1.5						0.6645	0.6642	0.6544	1.01e-02
		2						0.6712	0.6709	0.6617	9.50e-03
0.3	0.1	1	0.8					0.6503	0.6500	0.6338	1.65e-02
			1					0.6483	0.6480	0.6275	2.08e-02
			1.5					0.6440	0.6437	0.6104	3.36e-02
0.3	0.1	1	0.5	0.4				0.6541	0.6538	0.6433	1.08e-02
				0.6				0.6549	0.6546	0.6443	1.06e-02
				1				0.6562	0.6562	0.6462	1.00e-02
0.3	0.1	1	0.5	0.3	0.8			0.6541	0.6538	0.6433	1.08e-02
					1			0.6544	0.6545	0.6437	1.07e-02
					1.5			0.6553	0.6568	0.6447	1.06e-02
0.3	0.1	1	0.5	0.3	0.5	0.7		0.5384	0.5397	0.5205	1.79e-02
						0.8		0.5775	0.5784	0.5631	1.44e-02
						1.4		0.7906	0.7914	0.7841	6.50e-03
0.3	0.1	1	0.5	0.3	0.5	1	0.6	0.6784	0.6789	0.6673	1.11e-02
							0.7	0.7040	0.7045	0.6918	1.22e-02
							0.8	0.7295	0.7300	0.7164	1.31e-02

$Ec = 0.3$, $Pe = 0.5$, $\lambda = 0.2$, $Nt = 0.1$, $s = 0.1$, $K_p = 0.5$, $\epsilon = 0.2$, $\sigma_1 = 0.3$, $Pr = 6.8$, $\beta_1 = 0.4$, $\beta_2 = 0.4$.

Fig. 3.1 exhibits the impact on velocity profile for rising value of M . It can be observed that enhancement in value of M causes the momentum boundary layer to reduce. This reduction in boundary layer is due to Lorentz force which produce more friction to the fluid.

Fig. 3.2 depicts the impact of Kp on the profile of velocity. It can be observed that the velocity of fluid is decreased as Kp is increased.

Fig. 3.3 elaborates the influence of Pr_0 on the temperature profile. It can be observed that

enhancement in Pr_0 reduces the thermal boundary layer. As greater values of Pr_0 signifies to lower thermal diffusivity which corresponds to decay in temperature profile.

Fig. 3.4 exhibits the influence of Rd on temperature distribution. Physically more heat is provided to the fluid for increasing values of radiation parameter Rd .

Fig. 3.5 interprets the influence of Ec on the distribution of temperature. We witness that rise in the value of Ec causes enhancement in the fluid temperature.

Fig. 3.6 and Fig. 3.7 are drawn to see the impact of ϵ and s on the profile of temperature. It can be noticed that temperature is dominant for the greater values of both ϵ and s .

Fig. 3.8 is constructed to see the impact of β_1 on temperature profile. An enhancement in Biot number β_1 produces more convection which causes the raise in the fluid temperature.

Fig. 3.9 is constructed to see the impact of δ on profile of concentration. $\phi(\eta)$ decreases for the escalating values of temperature difference parameter δ .

Fig. 3.10 exhibits the influence of E on concentration profile. It can be seen that for rising values of activation energy parameter E the concentration profile is raised.

Fig. 3.11 exhibits the impact of n on concentration profile. It is observed that rising values of n diminishes the concentration profile.

Fig. 3.12 is drawn to exhibit the effects of Schmidt number Sc on the concentration ditribution of nanoparticles. It is observed that elaborating values of Sc decreases the concentration profile.

Fig. 3.13 refers to the impact of σ_1 on the concentration distribution. For greater values of σ_1 the concentration profile is declined.

Fig. 3.14 portrays the impacts of concentrated Biot number β_2 on profile of concentration. $\phi(\eta)$ enhances for escalating values of β_2 .

Fig. 3.15 and Fig. 3.16 potrays that for the greater values of Peclet number Pe and bio convection Schmidt number Sb the microorganism profile is decayed.

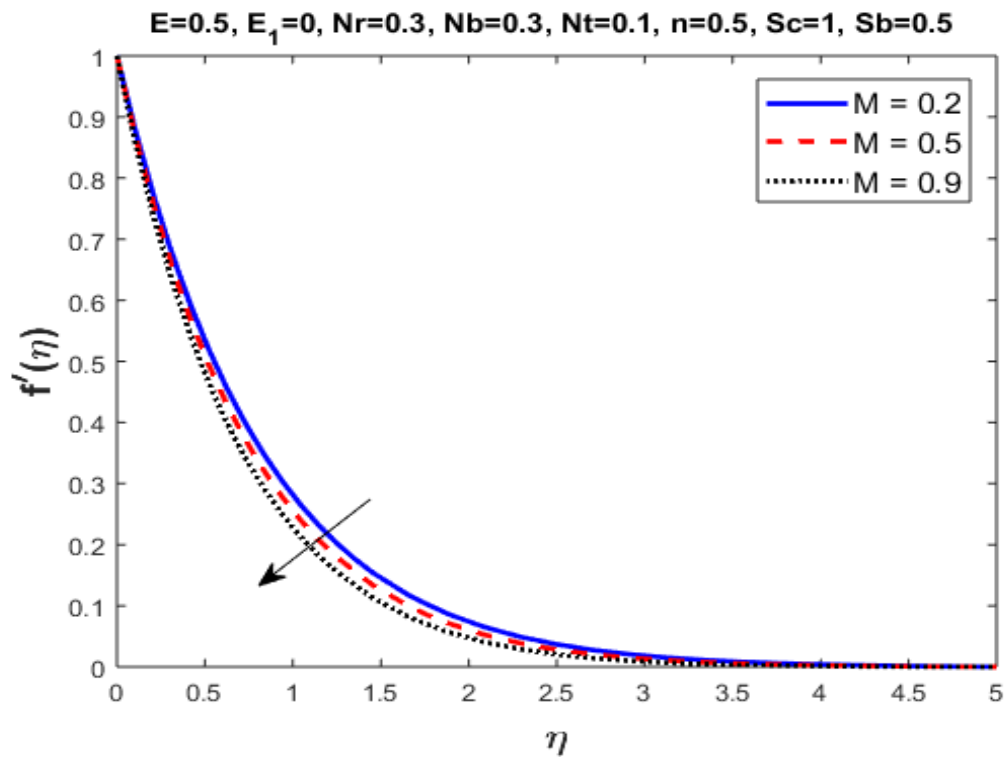


Figure 3.1: Computation of profile for velocity with respect to varied M .

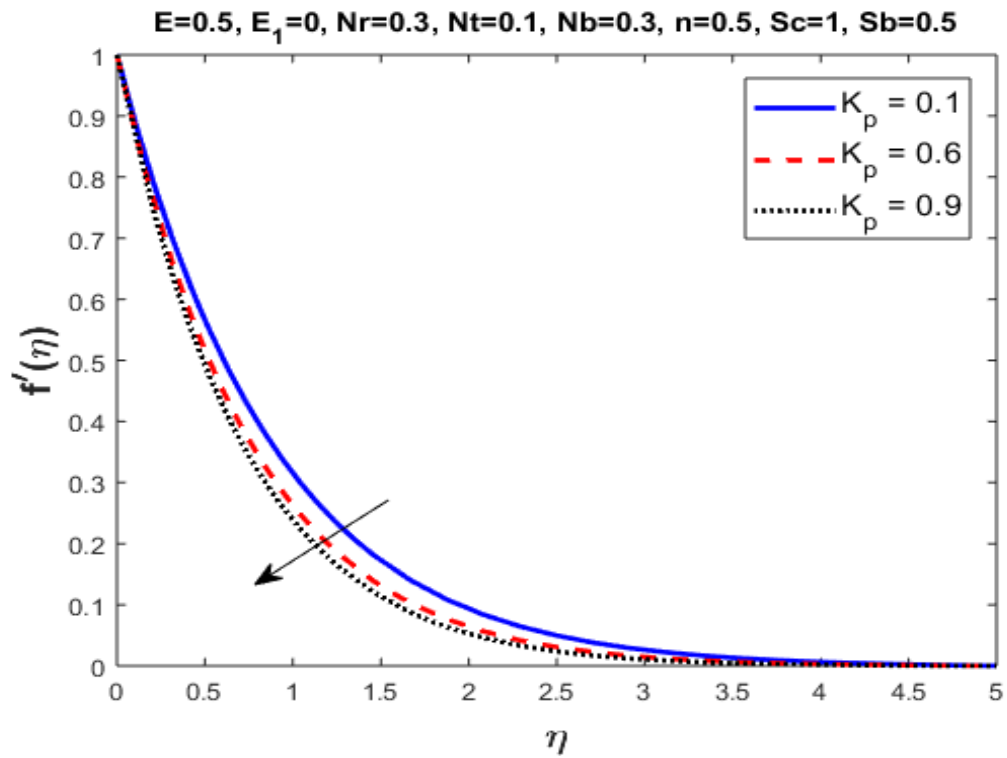


Figure 3.2: Computation of profile for velocity with respect to varied K_p .

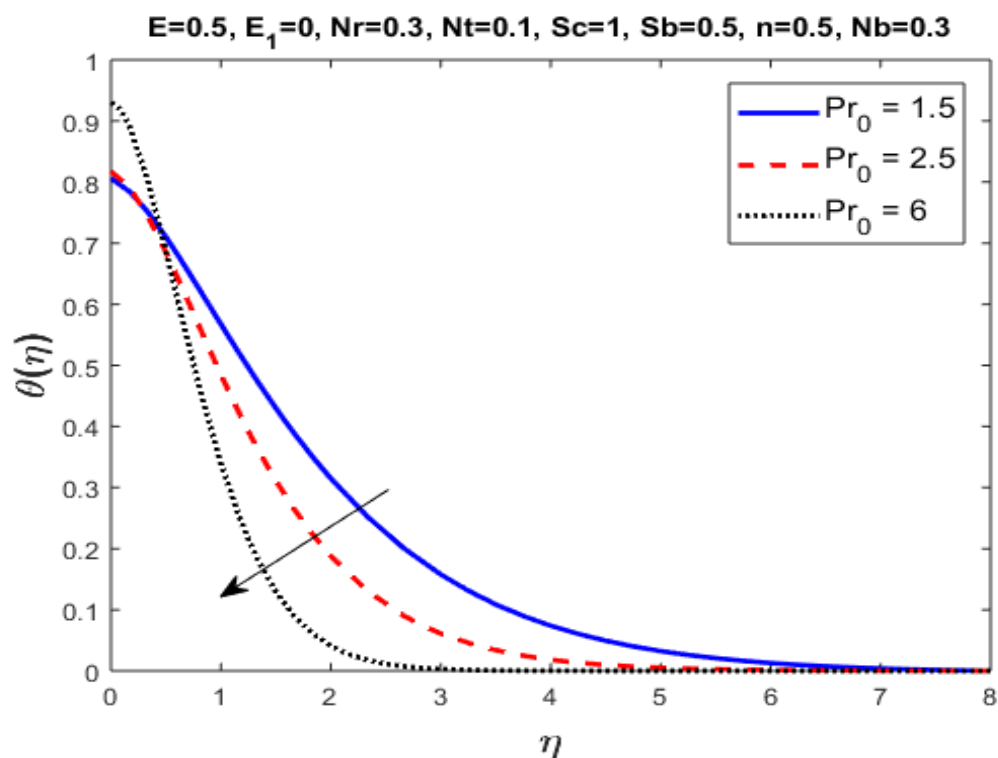


Figure 3.3: Computation of profile for temperature with respect to varied Pr .

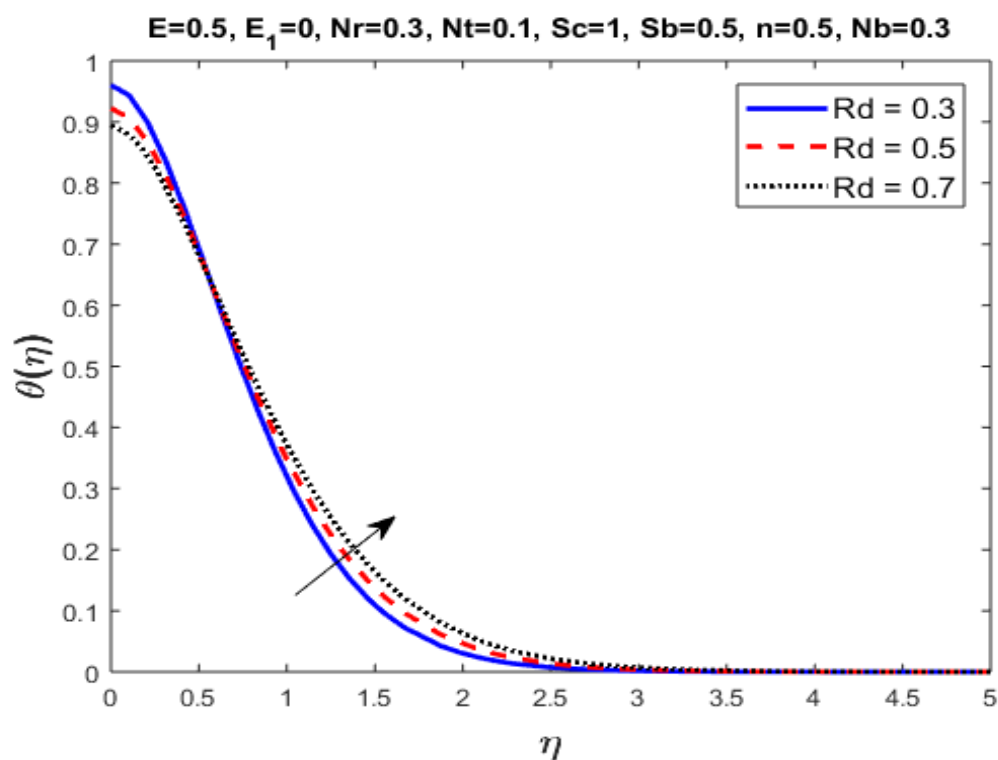


Figure 3.4: Computation of profile for temperature with respect to varied Rd .

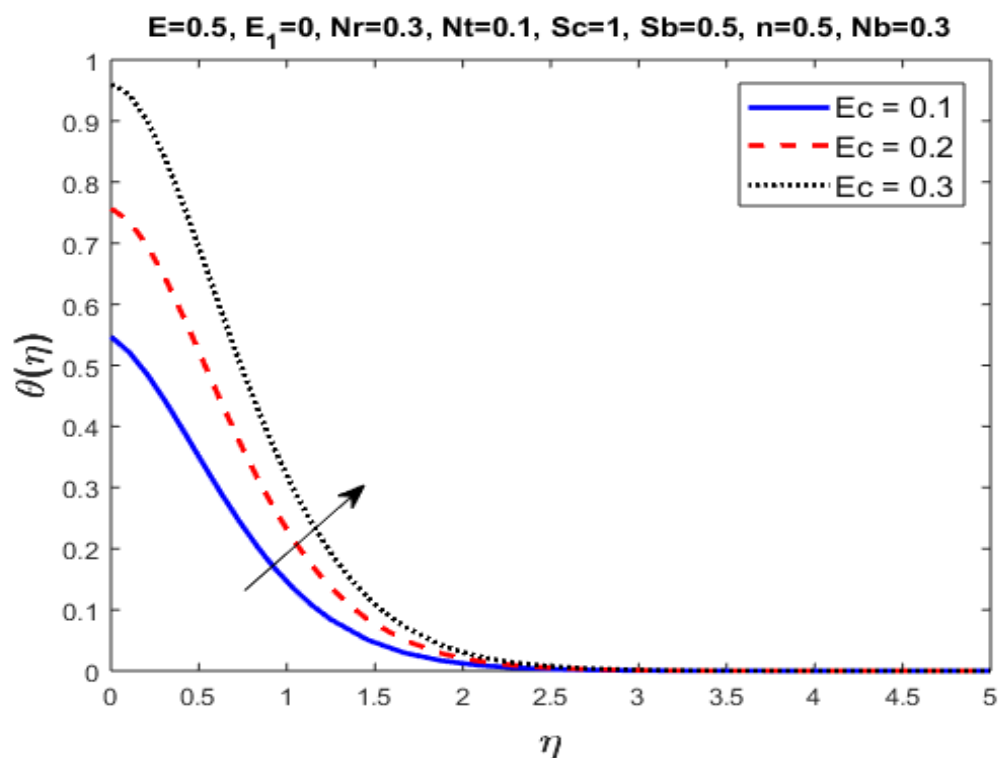


Figure 3.5: Computation of profile for temperature with respect to varied Ec .

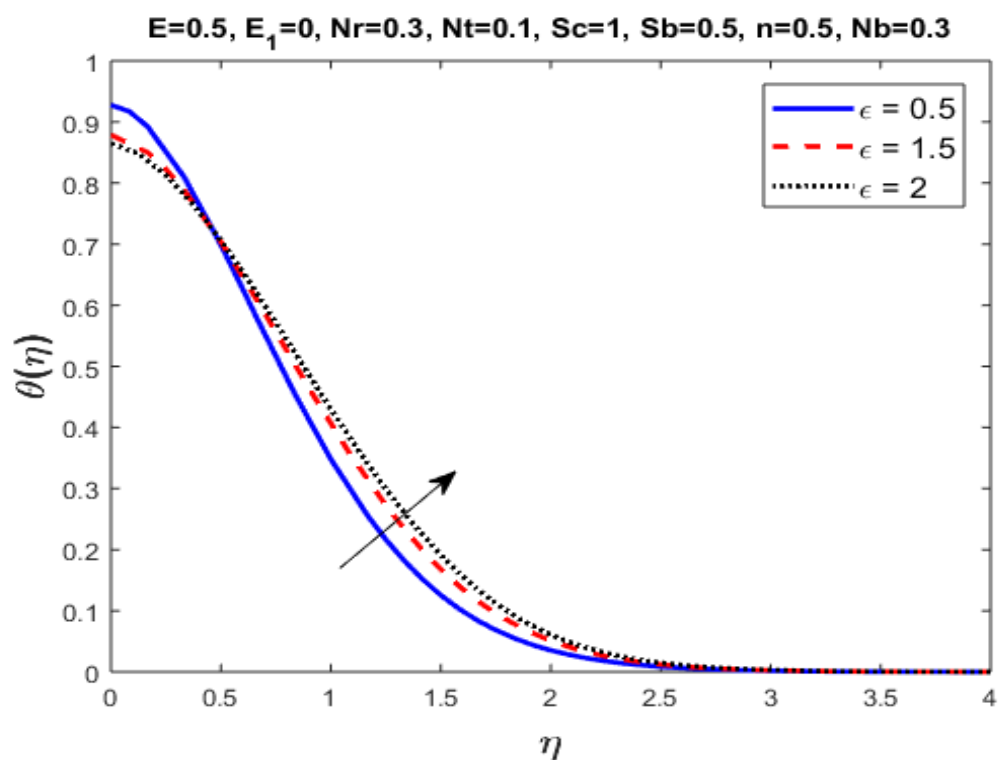


Figure 3.6: Computation of profile for temperature with respect to varied ϵ .

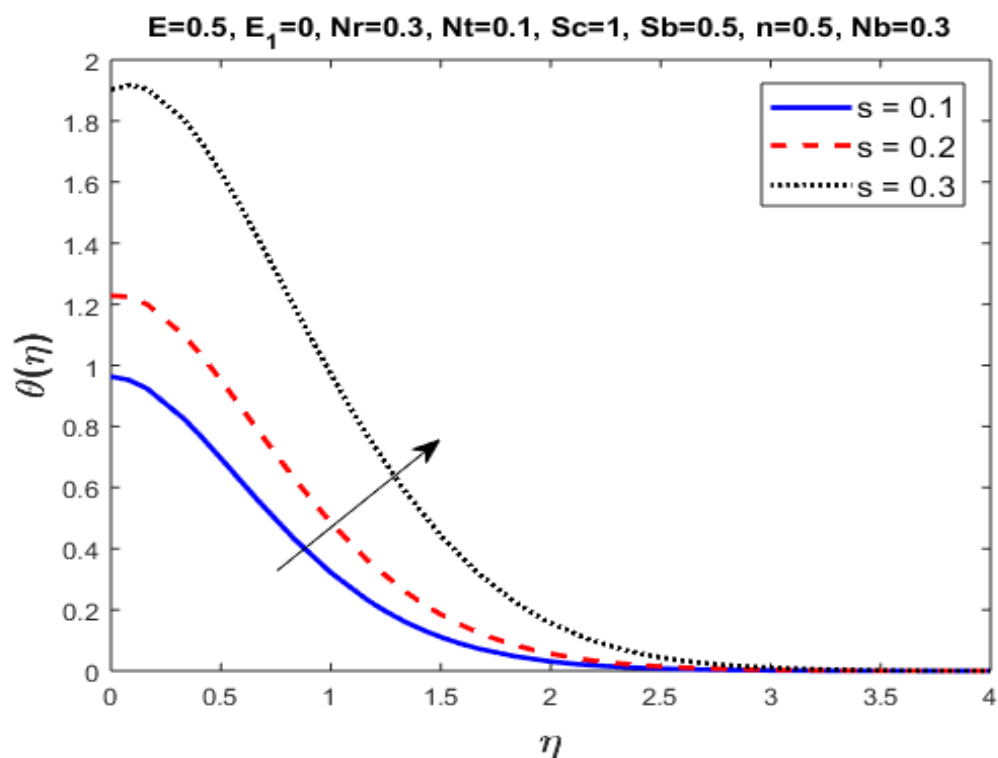


Figure 3.7: Computation of profile for temperature with respect to varied s .

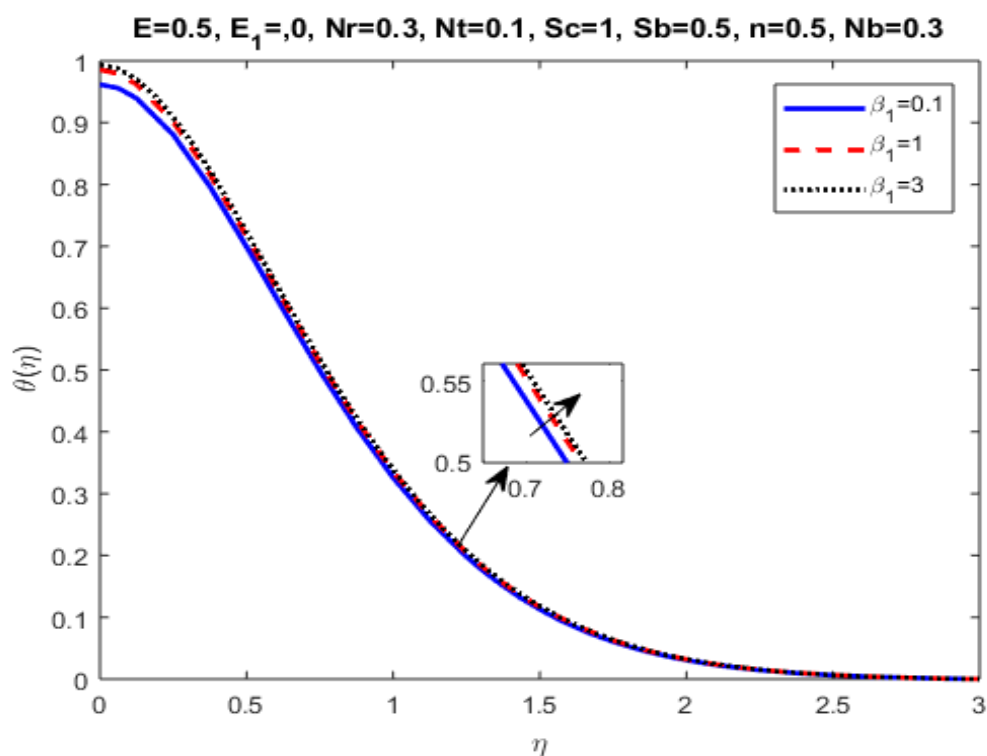


Figure 3.8: Computation of profile for temperature with respect to varied β_1 .

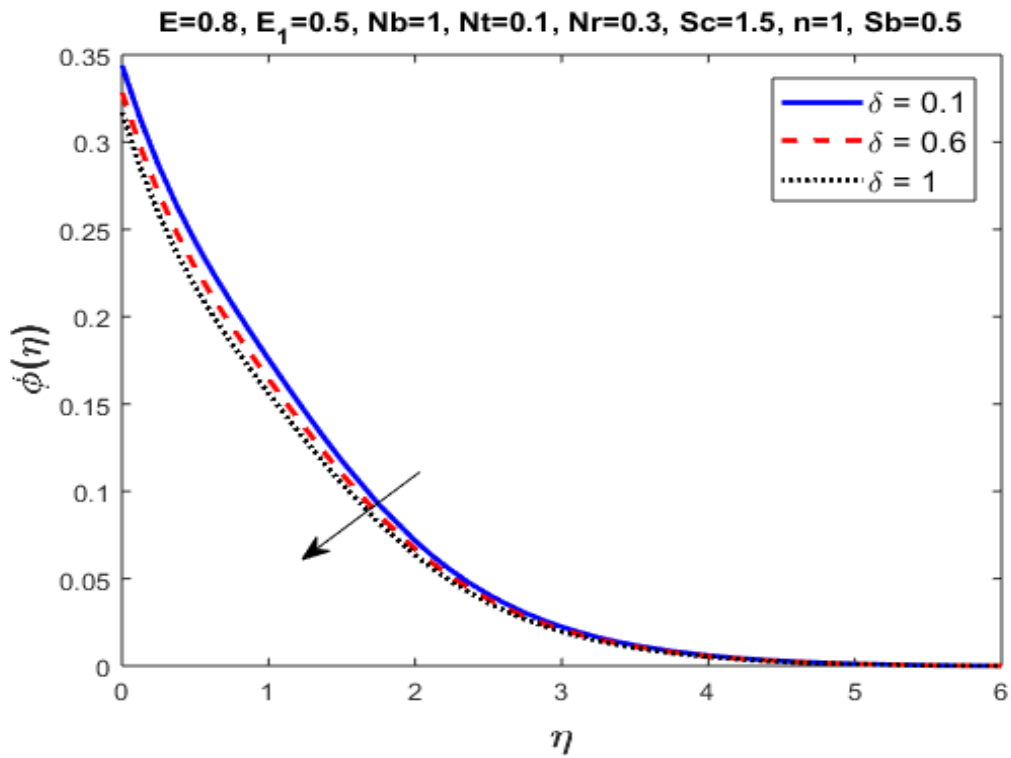


Figure 3.9: Computation of profile for concentration with respect to varied δ .

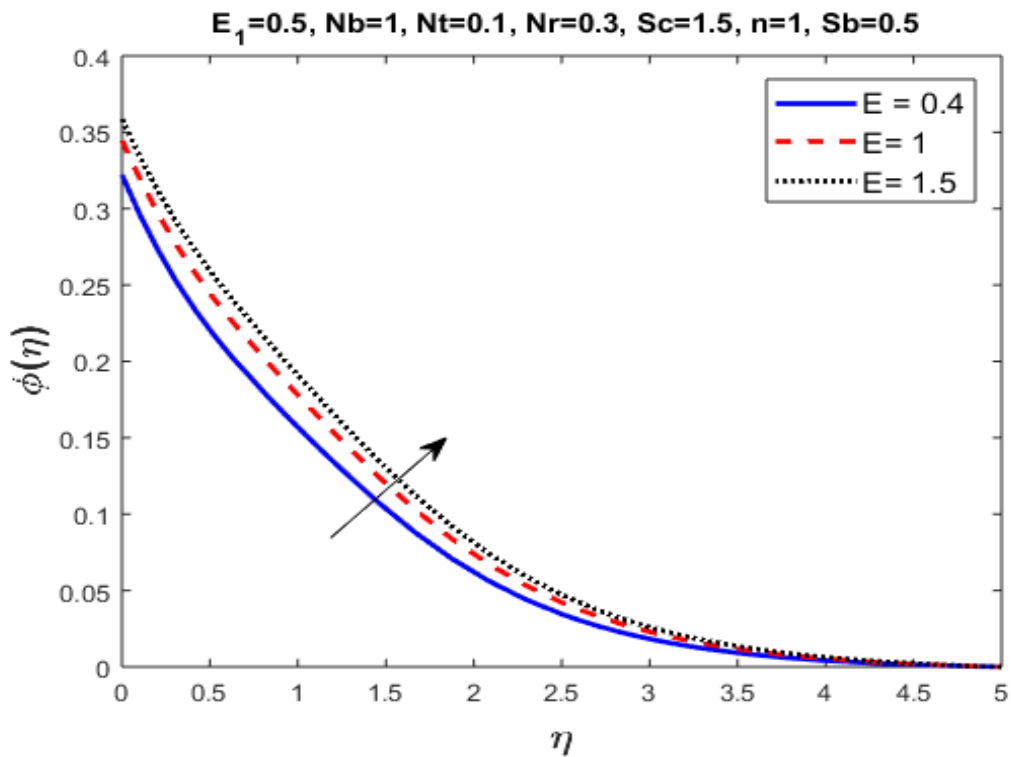


Figure 3.10: Computation of profile for concentration with respect to varied E .

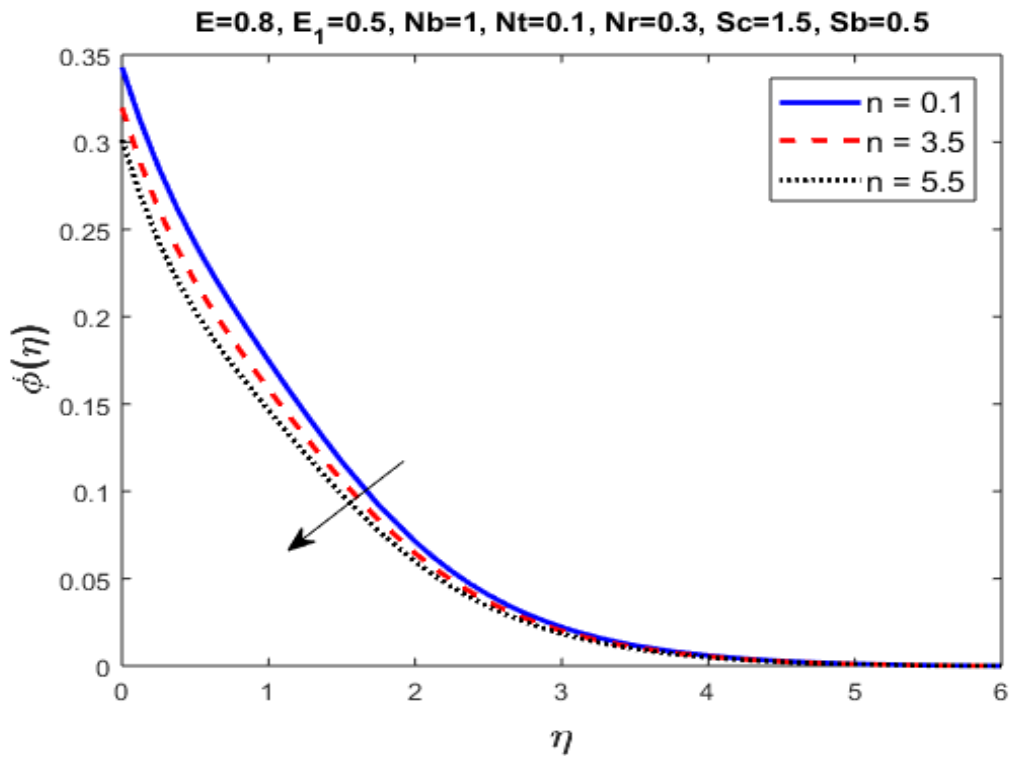


Figure 3.11: Computation of profile for concentration with respect to varied n .

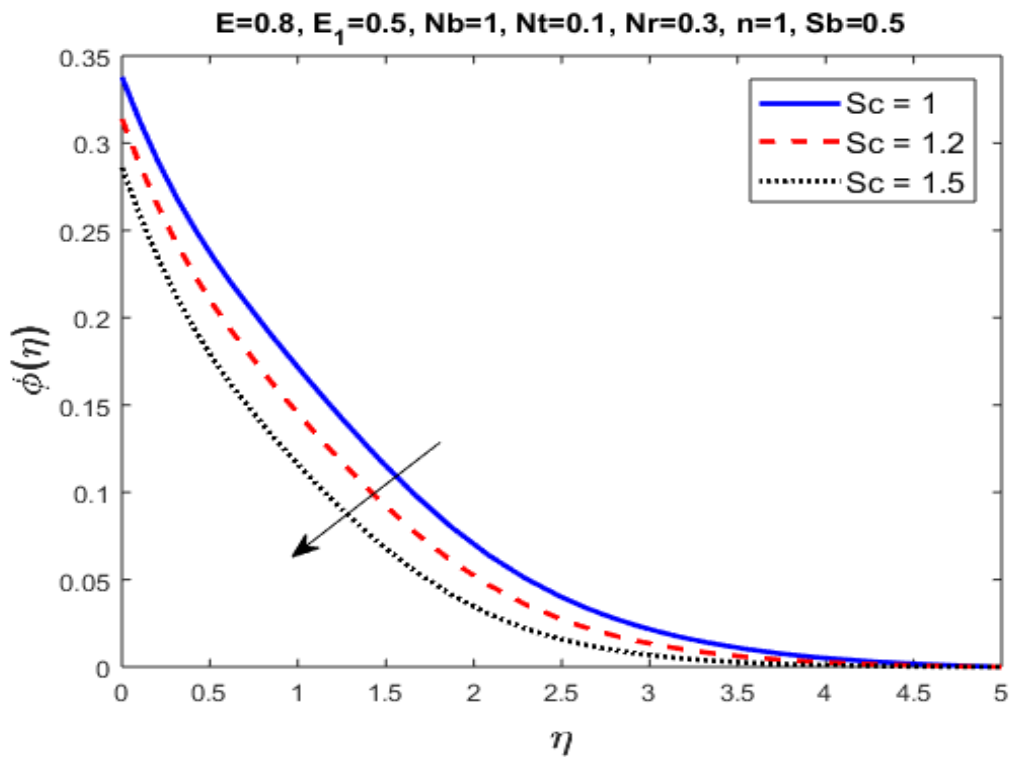


Figure 3.12: Computation of profile for concentration with respect to varied Sc .

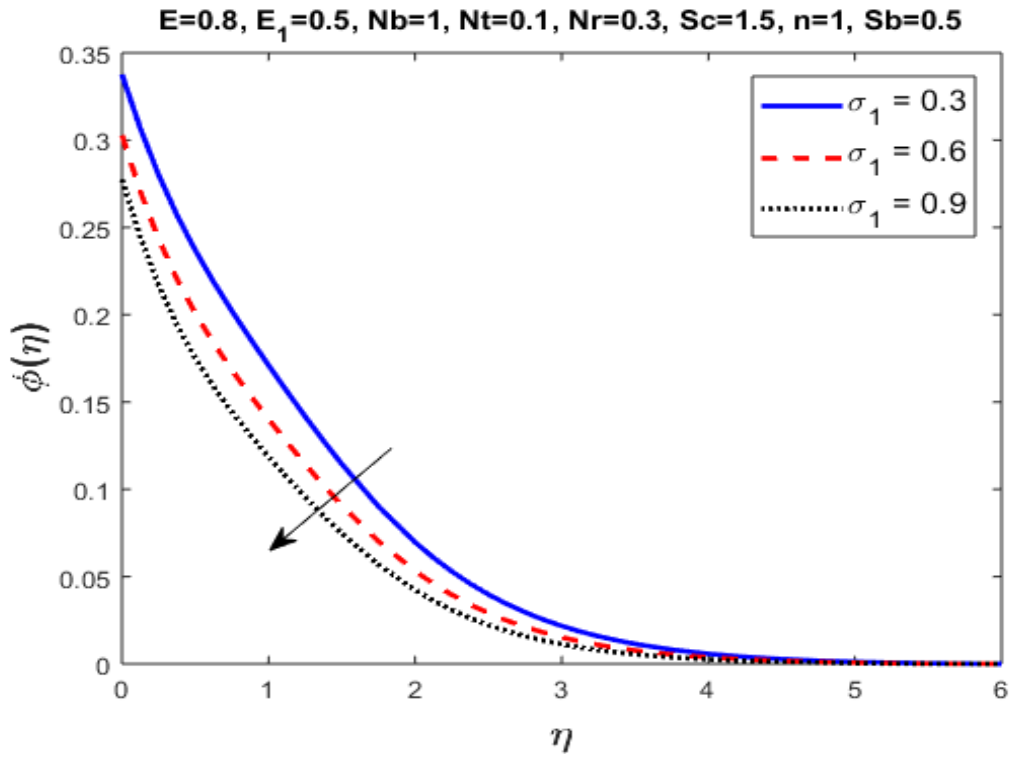


Figure 3.13: Computation of profile for concentration with respect to varied σ_1 .

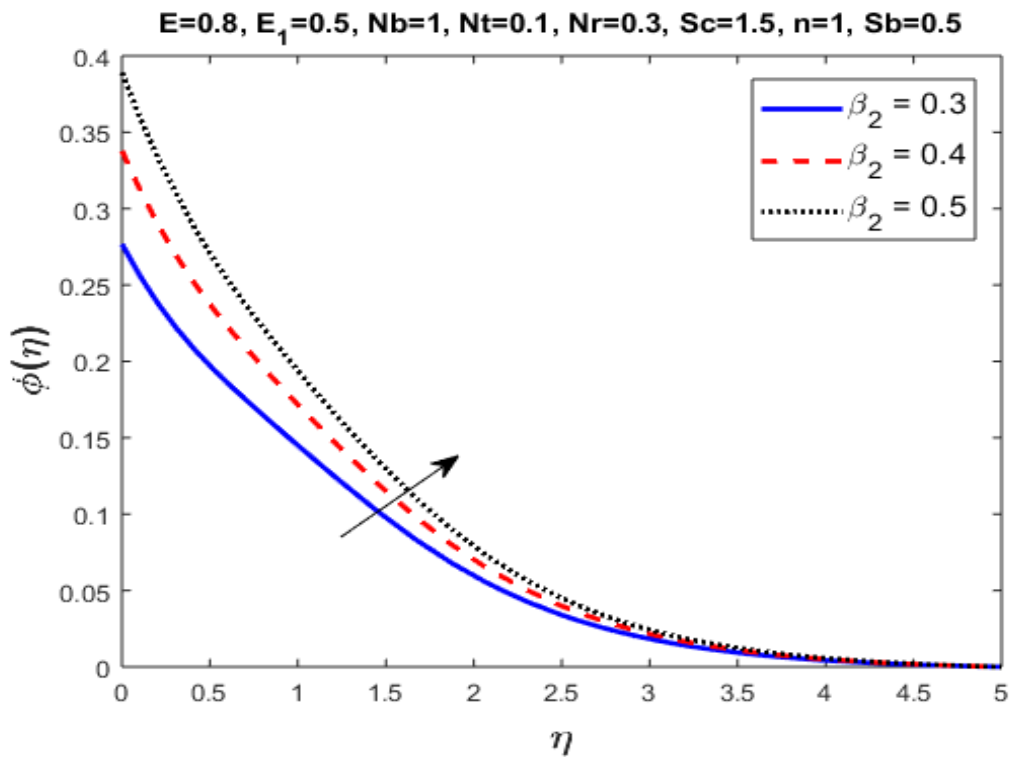


Figure 3.14: Computation of profile for concentration with respect to varied β_2 .

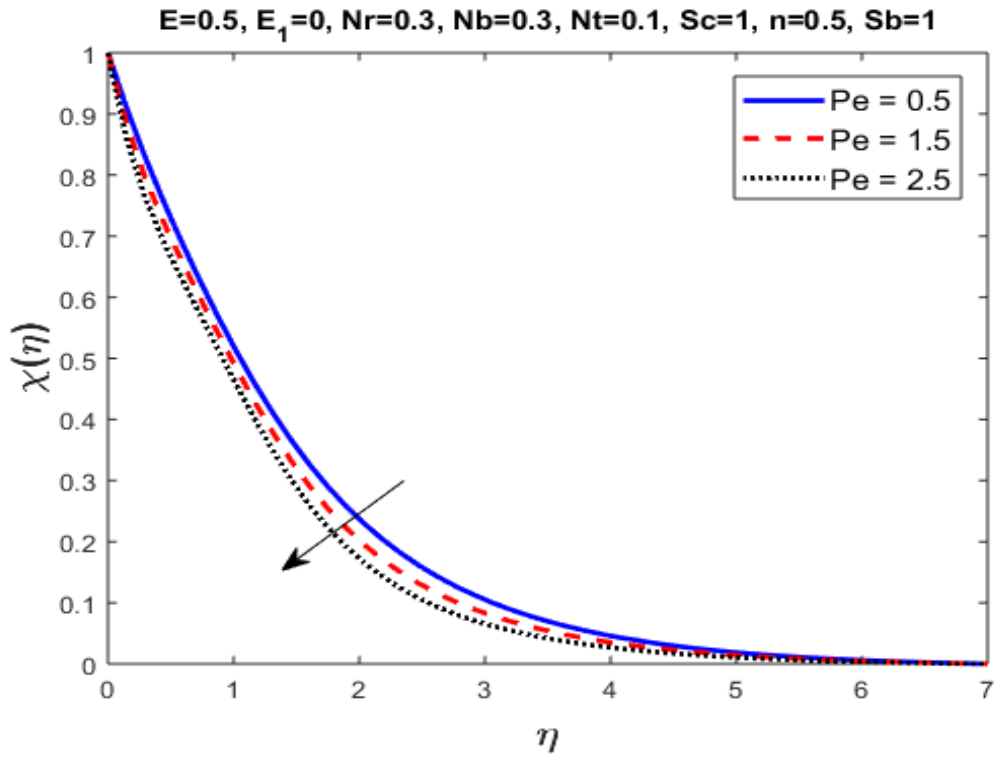


Figure 3.15: Analysis of microorganisms profile $\chi(\eta)$ for varied Pe .

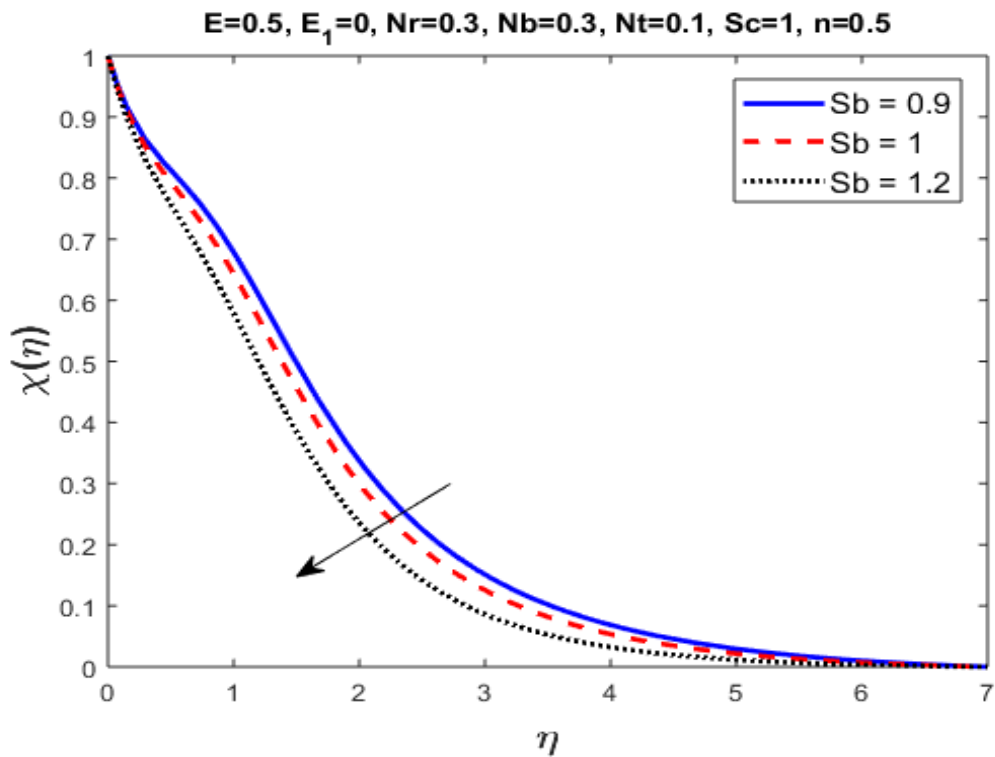


Figure 3.16: Analysis of microorganisms profile $\chi(\eta)$ for varied Sb .

Chapter 4

Conclusion

The thesis is primarily divided in three chapters. In the first chapter, a brief historical background is given along with basic definitions of fluid and its classes like Newtonian and non-Newtonian fluids. The various properties of fluid flow like compressible, incompressible, steady, unsteady and MHD flow is also explained. The conservation laws of mass, momentum and energy are also described. Dimensionless parameters like Reynolds number, Prandtl number and Eckert number are briefly mentioned. Lastly, the numerical methods including *bvp4c*, Shooting method and FEM are discussed.

In chapter two, we reviewed the problem of second grade fluid flow over a stretching sheet under the influence of buoyancy force and its impact on heat and mass transfer and solute distributions. The partial differential equations are converted into ODEs using the similarity variables. The ODEs are subsequently solved by using the MATLAB *bvp4c* solver. The results are plotted and presented in tabular form. The influence of dimensionless parameters on profiles of velocity, concentration and temperature is graphically represented. Similarly, dimensionless parameters behaviour subject to the various parameters is tabulated.

In chapter three, we explored the extended problem of impact of Arrhenius activation energy on EMHD mixed convection and heat transfer flow of bionanofluid in porous medium with radiative heat transfer while considering variable thermal conductivity over a non-linearly stretching sheet. The governing equations were transformed into ODEs using similarity variable. Following the transformation the FEM method, shooting method and *bvp4c* was applied using MATLAB. The results obtained using FEM were in excellent agreement with the results acquired by using other numerical methods. The results attained for the influence of various parameters on the dimensionless parameters like density of motile microorganisms etc. are tabulated. Graphical representation is also provided for impact of parameters on velocity, temperature, solute distribution and motile microorganisms. Few of the notable findings are:

- The increasing values of M magnetic parameter and porosity parameter exhibited by K_p

slow down the fluid velocity.

- The rising values of Rd radiation parameter, Biot number β_1 , Eckert number Ec , thermal conductivity parameter ϵ and s rises the fluid temperature. While temperature profile lowers down for growing values of Pr_0 .
- The concentration of nanoparticle is enhanced for rising values of activation energy E . While concentration of boundary layer reduces for large values of temperature difference parameter δ , chemical reaction parameter σ_1 and Sc Schmidt number .
- The microorganisms profile is declined for higher values Peclet number Pe .
- The skin friction coefficient is growing for various values of M magnetic parameter.
- For varied Rd and Ec the local Nusselt number enhances and lowers repectively.
- For increasing values of activation energy E , local Sherwood number is decreased and it is increased for rising values of temperature difference parameter δ .
- The density of motile microorganisms is increasing for raising value of Peclet number Pe .

Bibliography

- [1] Choi, S. US, and Jeffrey A. Eastman. Enhancing thermal conductivity of fluids with nanoparticles. No. ANL/MSD/CP-84938; CONF-951135-29. Argonne National Lab.(ANL), Argonne, IL (United States), 1995.
- [2] Buongiorno, Jacopo. "Convective transport in nanofluids." (2006): 240-250.
- [3] Gupta, P. S., and A. S. Gupta. "Heat and mass transfer on a stretching sheet with suction or blowing." *The Canadian journal of chemical engineering* 55, no. 6 (1977): 744-746.
- [4] Crane, Lawrence J. "Flow past a stretching plate." *Zeitschrift für angewandte Mathematik und Physik ZAMP* 21, no. 4 (1970): 645-647.
- [5] Das, K. "Impact of thermal radiation on MHD slip flow over a flat plate with variable fluid properties." *Heat and Mass Transfer* 48, no. 5 (2012): 767-778.
- [6] Chen, C-H. "Laminar mixed convection adjacent to vertical, continuously stretching sheets." *Heat and Mass transfer* 33, no. 5 (1998): 471-476.
- [7] Mabood, Fazle, Taseer Muhammad, M. K. Nayak, Hassan Waqas, and O. D. Makinde. "EMHD flow of non-Newtonian nanofluids over thin needle with Robinsons condition and Arrhenius pre-exponential factor law." *Physica Scripta* 95, no. 11 (2020): 115219.
- [8] Rasouli, M. R., A. Abouei Mehrizi, and A. Lashkaripour. "Numerical study on low reynolds mixing oft-shaped micromixers with obstacles." *Transp Phenom Nano Micro Scales* 3, no. 2 (2015): 68-76.
- [9] Kuznetsov, Andrey V. "Nanofluid bioconvection in water-based suspensions containing nanoparticles and oxytactic microorganisms: oscillatory instability." *Nanoscale research letters* 6, no. 1 (2011): 100
- [10] Uddin, M. J., W. A. Khan, S. R. Qureshi, and O. Anwar Baig. "Bioconvection nanofluid slip flow past a wavy surface with applications in nano-biofuel cells." *Chinese Journal of Physics* 55, no. 5 (2017): 2048-2063.

- [11] Aziz, A., W. A. Khan, and I. Pop. "Free convection boundary layer flow past a horizontal flat plate embedded in porous medium filled by nanofluid containing gyrotactic microorganisms." *International Journal of Thermal Sciences* 56 (2012): 48-57.
- [12] Mustafa, M., Junaid Ahmad Khan, T. Hayat, and A. Alsaedi. "Buoyancy effects on the MHD nanofluid flow past a vertical surface with chemical reaction and activation energy." *International Journal of Heat and Mass Transfer* 108 (2017): 1340-1346.
- [13] Khan, Umair, A. Zaib, Ilyas Khan, and Kottakkaran Sooppy Nisar. "Activation energy on MHD flow of titanium alloy (Ti_6Al_4V) nanoparticle along with a cross flow and streamwise direction with binary chemical reaction and non-linear radiation: Dual Solutions." *Journal of Materials Research and Technology* 9, no. 1 (2020): 188-199.
- [14] Makinde, O. D., and I. L. Animasaun. "Bioconvection in MHD nanofluid flow with nonlinear thermal radiation and quartic autocatalysis chemical reaction past an upper surface of a paraboloid of revolution." *International Journal of Thermal Sciences* 109 (2016): 159-171.
- [15] Andersson, Helge I., Olav R. Hansen, and Bjorn Holmedal. "Diffusion of a chemically reactive species from a stretching sheet." *International Journal of Heat and Mass Transfer* 37, no. 4 (1994): 659-664.
- [16] Petrilă, Titus, and Damian Trif. *Basics of fluid mechanics and introduction to computational fluid dynamics*. Vol. 3. Springer Science & Business Media, 2004.
- [17] Young, D. F., Munson, B. R., Okiishi, T. H., , Huebsch, W. W. *A Brief Introduction To Fluid Mechanics*. John Wiley , Sons, (2010).
- [18] Yunus, A. Cengel. *Fluid Mechanics: Fundamentals And Applications (Si Units)*. Tata McGraw Hill Education Private Limited, 2010.
- [19] Nguyen, Nam-Trung. *Micromixers: fundamentals, design and fabrication*. William Andrew, 2011.
- [20] Anwar, Talha, Poom Kumam, Dumitru Baleanu, Ilyas Khan, and Phatiphat Thounthong. "Radiative heat transfer enhancement in MHD porous channel flow of an Oldroyd-B fluid under generalized boundary conditions." *Physica Scripta* 95, no. 11 (2020): 115211.
- [21] Fagbenle, R. O., Olaleye Michael Amoo, Ayodeji Falana, and Sufianu Aliu, eds. *Applications Of Heat, Mass And Fluid Boundary Layers*. Woodhead Publishing Limited, 2020.
- [22] Frank, M. *Fluid Mechanics Fourth Edition*. McGraw-Hill, 2017.

- [23] Shafiq, Anum, Ghulam Rasool, Chaudry Masood Khaliq, and Sohail Aslam. "Second grade bioconvective nanofluid flow with buoyancy effect and chemical reaction." *Symmetry* 12, no. 4 (2020): 621.
- [24] Waqas, H., Khan, S.U., Hassan, M., Bhatti, M.M. and Imran, M., 2019. Analysis on the bioconvection flow of modified second-grade nanofluid containing gyrotactic microorganisms and nanoparticles. *Journal of Molecular Liquids*, 291, p.111231.
- [25] Prasannakumara, B. C., B. J. Gireesha, M. R. Krishnamurthy, and K. Ganesh Kumar. "MHD flow and nonlinear radiative heat transfer of Sisko nanofluid over a nonlinear stretching sheet." *Informatix in Medicine Unlocked* 9 (2017): 123-132.
- [26] Khan, Masood, Rabia Malik, Asif Munir, and Waqar Azeem Khan. "Flow and heat transfer to Sisko nanofluid over a nonlinear stretching sheet." *PLoS One* 10, no. 5 (2015): e0125683.
- [27] Prasad, K. V., Dulal Pal, V. Umesh, and NS Prasanna Rao. "The effect of variable viscosity on MHD viscoelastic fluid flow and heat transfer over a stretching sheet." *Communications in Nonlinear Science and Numerical Simulation* 15, no. 2 (2010): 331-344.
- [28] Na, Tsung Yen. "Computational methods in engineering boundary value problems." (1979).
- [29] Kiusalaas, Jaan. *Numerical methods in engineering with MATLAB*. Cambridge university press, 2005.
- [30] Kierzenka, Jacek, and Lawrence F. Shampine. "A BVP solver based on residual control and the Matlab PSE." *ACM Transactions on Mathematical Software (TOMS)* 27, no. 3 (2001): 299-316.
- [31] Goyal, Mania, and Rama Bhargava. "Boundary layer flow and heat transfer of viscoelastic nanofluids past a stretching sheet with partial slip conditions." *Applied Nanoscience* 4, no. 6 (2014): 761-767.
- [32] Reddy Gorla, Rama Subba, and Ibrahim Sidawi. "Free convection on a vertical stretching surface with suction and blowing." *Applied Scientific Research* 52, no. 3 (1994): 247-257.